

J 20 419 F

*A Publication
for the Radio-Amateur
Especially Covering VHF,
UHF and Microwaves*

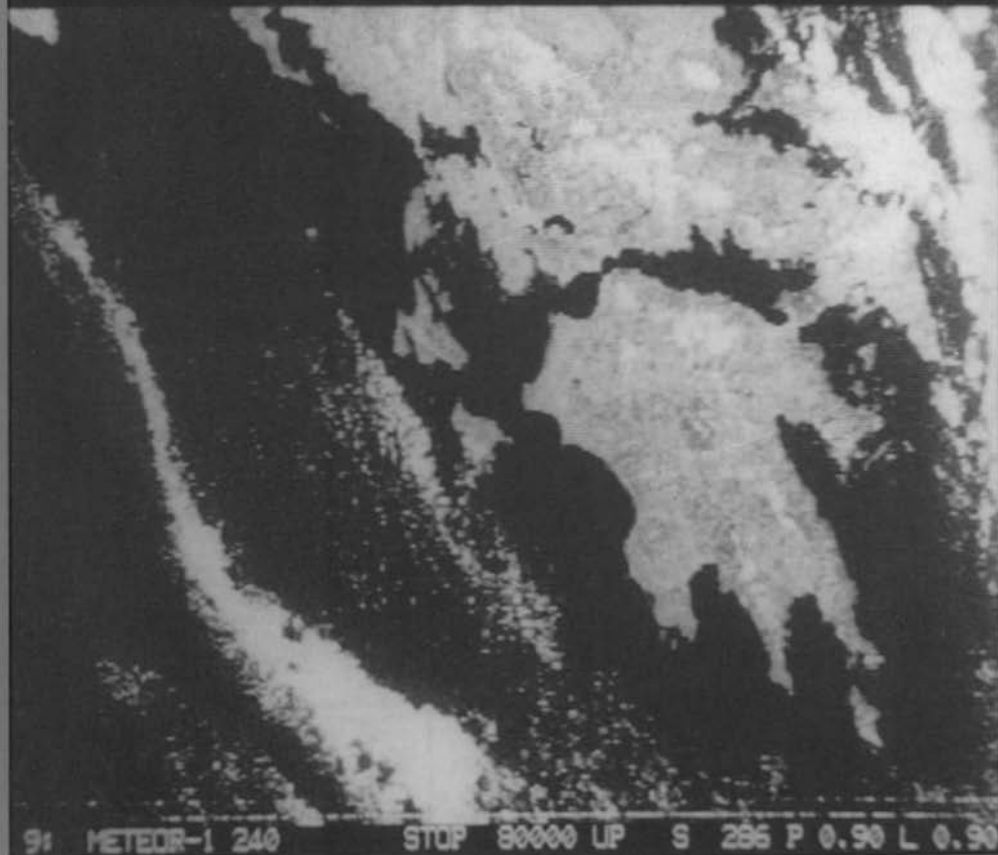


VHF

communications

Volume No. 21 · Winter · 4/1989 · DM 7.50

DSP Software TRACK & APT: Demod., Synch. & Enhancement





VHF communications

A Publication for the Radio Amateur
Especially Covering VHF, UHF, and Microwaves

Volume No. 21 · Winter · Edition 4/1989

Published by: TERRY BITTAN OHG, P.O.Box 80,
Jahnstraße 14, D-8523 BAIERSDORF
Fed. Rep. of Germany
Telephone (9133) 47-0 Telex 629 887
Telefax 0 91 33-47 18
Postgiro Nbg. 30455-858

Publishers: TERRY BITTAN OHG

Editors: Corrie Bittan
Colin J. Brock (Assistant)

Translator: Colin J. Brock, G 3 ISB/DJ Ø OK

**Advertising
manager:** Corrie Bittan

**VHF
COMMUNICATIONS**

The international edition of the German publication UKW-BERICHTE is a quarterly amateur radio magazine especially catering for the VHF / UHF / SHF technology. It is published in Spring, Summer, Autumn and Winter. The 1990 subscription price is DM 27.00 or national equivalent per year. Individual copies are available at DM 7.50 or equivalent each. Subscriptions, orders of individual copies, purchase of PC-boards and advertised special components, advertisements and contributions to the magazine should be addressed to the national representative, or – if not possible – directly to the publishers.

©Verlag
UKW-BERICHTE

All rights reserved. Reprints, translations, or extracts only with the written approval of the publisher.

Printed in the Fed. Rep. of Germany by R. Reichenbach KG Kreilingstr. 39 · 8500 Nuernberg.

We would be grateful if you would address your orders and queries to your representative.

Representatives

Austria
Verlag UKW-BERICHTE, Terry D. Bittan
POB 80, D-8523 Baiersdorf / W. Germany

Australia
W.I.A. P.O. Box 300, South Caulfield, 3162 VIC,
Phone 5285962

Belgium
HAM INTERNATIONAL, Brusselssesteenweg 428,
B-9218 GENT, PCR 000-1014257-25,
Tel. 00-32-91-312111

Denmark
Halskov Electronic, OZ 7 LX, Sigersted gamle Skole,
DK-4100 RINGSTED, Tel. 03-616162, Giro 7 29 68 00

France
Christiane Miché, F 5 SM, SM Electronic,
20 bis, Avenue des Clairons, F-89000 AUXERRE
Tel. (86) 46 96 59

Finland
Peter Lytz, OH 2 AVP, Gesterbystingen 14 E 49
SF-02410 Kyrkslätt, Tel. 358/0/2 98 17 61
SRAT, PL 44
SF-00441 Helsinki, Tel. 358/0/5625973

Holland
DOEVEN-ELEKTRONIKA, J. Doeven, Schutstraat 58,
NL-7901 EE HOOGEVEEN, Tel. 05280-69679

Israel
Doron Jacobi 4Z4RG, P.O. Box 6382
HAIFA, Israel 31063

Italy
ADB ELETTRONICA di Lucchesi Fabrizio, IW 5 ADB,
Via del Cantone 714, 55100 Antraccoli (Lucca), Tel. 0583-952612

Luxembourg
TELECO, Jos. Faber, LX 1 DE, 5-9, Rue de la fontaine,
ESCH-SUR-ALZETTE, Tel. 53752

New Zealand
E. M. Zimmermann, ZL 1 AGQ, P. O. Box 31-261
Milford, AUCLAND 9, Phone 492-744

Norway
Henning Theg, LA 4 YG, Kjelaveien 30,
N-1370 ASKER, Postgirokonto 3 16 00 09

South Africa
HI-TECH BOOKS, P. O. Box 1142, RANDBURG,
Transvaal 2125, Tel. (011) 886-2020

Spain + Portugal
Julio A. Prieto Alonso, EA 4 CJ, MADRID-15,
Donoso Cortés 58 5-B, Tel. 243.83.84

Sweden
Lars Pattersson, SM 4 IVE, Pl. 1254, Smögården Talby,
S-71500 ODENSBACKEN, Tel. 19-50223, Pg. 914379-3

Switzerland
Terry Bittan, Schweiz, Kreditanstalt ZÜRICH,
Kto. 469.253-41; PSchKto. ZÜRICH 80-54.849
Leo Kälin, HB 9 CKL, Funktechnik
Alte Landstr. 175, CH 8708 Männedorf
Tel. 01-9203535

United Kingdom
Mike Wooding, G 6 IQM, 5 Ware Orchard
Barby, nr. Rugby, Warks CV23 8UF, Tel. 0788 890365

USA
Timekit, P. O. Box 22277,
Cleveland, Ohio 44122, Phone: (216) 464-3820

ISSN 0177-7505



Contents

Hans J. Hartfuss, DL 2 MDQ	Radio Astronomy for the VHF/UHF Radio Amateur	194 - 204
Peter Gerber, HB 9 BNI	Calculating the Sun and Moon's Kepler Elements	205 - 210
Joachim Berns, DL 1 YBL	24/23 cm-Band Linear Power Amplifier Module M 57762	211 - 215
Matjaž Vidmar, YT 3 MV	Digital Signal Processing Techniques for Radio Amateurs Part 4 b: Application Software	216 - 227
Hans Michl, Heilbronn	2.83 GHz DR-Oscillator	228 - 231
Roman Wesolowski, DJ 6 EP	9 cm-Band Tube PA Stage	232 - 241
Carsten Vieland, DJ 4 GC	Screw-Tuned Filter for the X-Band	242 - 246
Roy Hartkopf, VK 3 AOH	Shunt-Protected Power Supply	247 - 248
Werner Rahe, DC 8 NR	9 cm-Band Power-FET Linear Amplifier	249 - 254

Cover story

Our cover shows a picture from a USSR Weather Satellite in the METEOR-Series. As may be deduced from the data at the lower edge of the picture, it was demodulated, synchronized and processed with the YT 3 MV DSP-Computer.

VHF COMMUNICATIONS wishes all readers
a **Merry Christmas** and a **Happy and Prosperous New Year!**



UKWberichte

T. Bittan OHG · Jahnstr. 14 · P.O.Box 80 · D-8523 Baiersdorf

Tel. West Germany 9133 47-0. For Representatives see cover page 2



Hans J. Hartfuss, DL 2 MDQ

Radio Astronomy for the VHF/UHF Radio Amateur

Based on a Lecture given at the 1988 VHF/UHF Conference in Munich

There is hardly a radio amateur who is not acquainted with pictures of the huge astronomical radio telescopes. These range from the 100 m mirror of the Max-Planck institute at Effelsberg in Germany to the 300 m (approx.) Arecibo telescope located in a natural depression in Puerto Rico, to name only two of the biggest.

One has heard of the fantastic receivers employed using super-cooled pre-amplifiers, of the computers for antenna control and filtering the signal from the basic intrinsic noise generated by the receiving system. Radio signals from other stars, the interstellar material or signals from other galaxies, are received by these systems. Signals which have travelled for millions of years before they have impinged upon the Earth's surface.

One hears about the discovery of strange objects, of Quasars and Pulsars, burned-out stars and the discovery of carbon-dioxide molecules even in distant neighboring galaxies. A fantastic world of the universe as seen with the radio eye (1).

Only a few radio amateurs know, however, that they can also delve into this fascinating world, using their own equipment, even if the last named wonders will be denied them. But there is – apart from the Sun – a few further intra and extra-galactical signal sources whose radiations are sufficiently intense to be

observed by amateur means. The purpose of this article is to explain how this may be achieved. It will acquaint those interested with a few basic considerations and present him with some assessments and evaluations. These will assist in the decision of whether, or not, a further incursion into this area, is interesting enough to merit the trouble and expense.

1. HISTORICAL

It all started about 50 years ago when Karl Jansky, a radio engineer at the Bell laboratories in Holmdel, New Jersey, USA, was examining the interference to radio reception near the present-day 15 m band. His array comprised four two-element Quad antennas (2) rotatable in both the azimuth and horizontal planes. He found three natural interferences sources. These were distant and local thunderstorms and a constant noise which intensified when he directed his antenna towards Orion "The Hunter" constellation near the centre of the Milky Way. He was thus the first person to recognize radio emissions which originated from space even though it as in quite



a co-incident manner. The (optical) astronomers, however, displayed little interest, at first, in the fact that a new window had been opened to the universe which could be used to explore its wonders.

Interest was shown by an amateur astronomer, Grote Reber in Illinois, who was exited by Jansky's discovery. He constructed a 10 m parabolic mirror in the garden of his house and began to systematically search the heavens. At first, he had no success when he tried at 3.3 GHz and at 910 MHz but he heard what he was searching for on 160 MHz.

In 1944, he published the first radio map of the heavens i.e. as "seen" by a 160 MHz receiver. He found the strongest radio sources in Cassiopeia A, Cygnus A, Sagittarius etc in an almost continuously radiating celestial dome. The 160 MHz antenna had a beamwidth of approximately 12° which limited the detail on his map but the resolution was good enough to be able to identify individual objects.

Following the war, the young science was able to procure electronic equipment intended for military purposes and thereby received a tremendous fillip. This material included radar installations (Würzburg Giant etc.) and, of course, skilled radar technicians who made their experience available. The greatest activity in these post-war years was aroused in England and Australia but many more countries later developed experimental installations.

Two important discoveries in the rich history of Radio Astronomy should now be mentioned.

In 1951, the emission of galactic hydrogen, predicted in 1944, was discovered at a frequency of 1420.4056 MHz and whose spectral analysis led to the realization of the spiral nature of our own galaxy (3). Also, in 1964, workers at the Bell Laboratories using a sensitive receiver and a gigantic antenna installation at 7.3 cm, discovered the cosmic 2.7 K background, or residual radiation, whose existence tended to confirm, to a very high degree, the bigbang theory of the origin of the universe. The installation was only 3 km from the place where Jansky made his pioneering discoveries.

It should not be left unsaid, that when Jansky's original equipment was used 15 years later to try and emulate his findings, nothing could be heard. Unfortunately, the interference level in the band he was using had grown to such proportions that the radiations from the Milky Way were completely obscured.

2. RADIO EMISSIONS

Radio emissions, such as those which may be received from space, have the random character of noise in a resistor or from an amplifier. It is, in general, wideband inasmuch that it can be observed over all the frequencies familiar to amateurs i.e. 20 to 20,000 MHz. Its special frequency characteristic, however, betrays something of its origins. Three mechanisms come into play here. The radiation from a black body, the thermal radiation of an ionized gas and the synchrotron radiation.

Every body having a finite temperature, emits electro-magnetic radiations over a large radio-frequency spectrum. "Continuous radiation" is spoken of as opposed to "linear radiation" by which the emissions are radiated on one or several discrete frequencies. If the body is ideally black, i.e. it absorbs all the energy at all wavelengths, then its emissions, or more exactly, its spectral energy density, may be found by means of a well-known formula. This complicated formula was evolved by Max Planck at the beginning of this century. This quantifies the rule, that the hotter the body is the stronger are its emissions in all parts of the spectrum. That spectrum has a particular maximum, which, with rising body temperature is shifted into the short-wave regions. The emission-maximum of a body at room temperature, 300 K, lies in the infrared spectrum. If the body is cooled to the region of a few degrees Kelvin the emission maximizes in the millimetre band. The Sun too, behaves almost as a black radiator over the whole frequency spectrum with the emission maximum occurring in the green-yellow spectrum i.e. $0.5 \mu\text{m}$. From

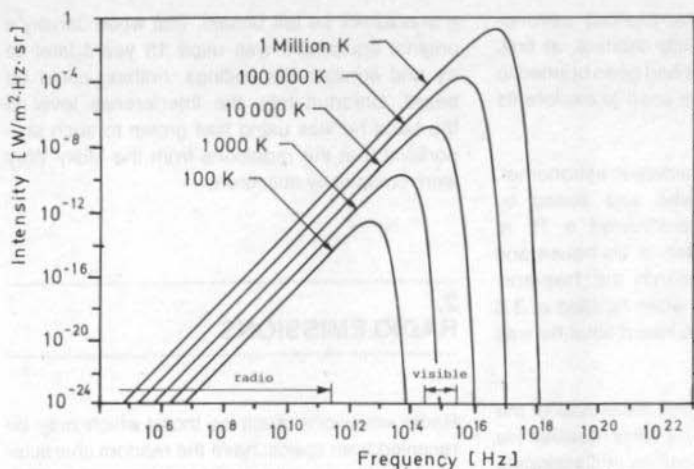


Fig. 1:
Black-body spectrum
at various radiator
temperatures

this information, the surface temperature of the Sun's photosphere may be calculated to be about 5800 K.

As shown in **fig. 1**, the radiation maximum for the given temperature parameter takes place at shorter wavelengths than those belonging to the classical radio spectrum. The total radio wave spectrum lies in the rising, linear portion of the individual characteristic. In this part of the emission spectrum, the Rayleigh-Jeans law is used to describe the classical Planck law for the long-wave emission spectrum. The specific intensity I_λ of the black body can then be given for a polarization direction by: -

$$I_\lambda = \frac{kT}{\lambda^2} \quad (\text{W/m}^2 \times \text{Hz} \times \text{rads}) \quad (1)$$

where T = the absolute temperature of the body
 λ = wavelength
 k = Boltzmann's constant =
 $= 1.38 \times 10^{-23} \text{ J/K}$

If this is then multiplied by the space angle Ω_Ω , under which the source under observation appears, the flux S , given in Watts per square metre and per Herz bandwidth, can be obtained.

As the radiation flux of radio-astronomic sources is very small, a flux unit of $10^{-26} \text{ W/m}^2 \text{ Hz}$ has been chosen in honour of the radio astronomer Jansky and is shorted to the "Jy".

The equation (1) is only valid for the case of the ideal black radiating body. The equation is used for the definition of an equivalent radiation temperature whereby an observed flux from any non-ideal, or from the superimposition of several radiators, will result in the same flux as that calculated from an equivalent black radiator temperature according to eq. 1.

Whilst most bodies in the solar system are thermal radiators, many sources display quite a different dependence from that typical of a black body radiator. Quite a different mechanism is clearly the reason. One example of this, is the Synchrotron radiation of high energy electrons which leads to a linear emission relationship with wavelength. To delve further into the various mechanisms would be quite inappropriate for an article of this scope. **Fig. 2** gives examples of the frequency dependence of the flux of a few sources.

Besides these continuous radiations, there are linear radiations. The most prominent of these, is



that mentioned in the beginning of the article, namely, the hydrogen line near the 23 cm band. Neutral hydrogen is found in the Galaxy with a density of approximately one atom per cubic centimeter. The expansion of the interstellar space is, however, so great that the total amount of radiation from the depths of space is sufficient to be observable.

From the linear profile, and the frequency shift of this radio line due to the Doppler effect, further important conclusions may be drawn concerning the structure of the Galaxy.

3. DISTRIBUTION PATHS

Whilst the greatest obstacle for optical observations is the absorption of the light rays by the interstellar dust particles and, of course, the Earth's atmospheric conditions, the strength of astronomical radio signals is determined by both the absorption characteristics of ionosphere and atmosphere. Their characteristics lead to the existence of a radio window, an open portion of the spectrum from 1 cm to 10 m (fig. 3) which allows the signals to pass through with minimum attenuation.

The long-wave end of this window will be familiar to the radio amateur as being influenced by the ionosphere, whilst the limit of the shorter-wavelength end, in the mm-range, is determined

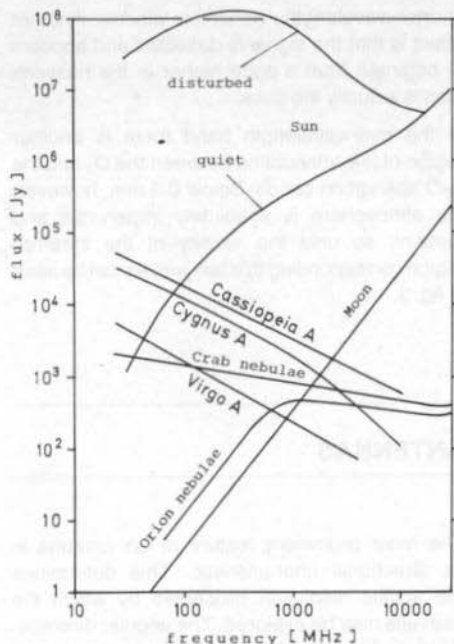


Fig. 2: The flux of the strongest sources as a function of frequency

by absorption of the signals by water (H₂O) and to a lesser extent by other molecules such as oxygen O₂. However, within this window the signal strength can also be affected by a variety of afflictions. Among these, rain and fog make a noticeable effect upon the attenuation of the

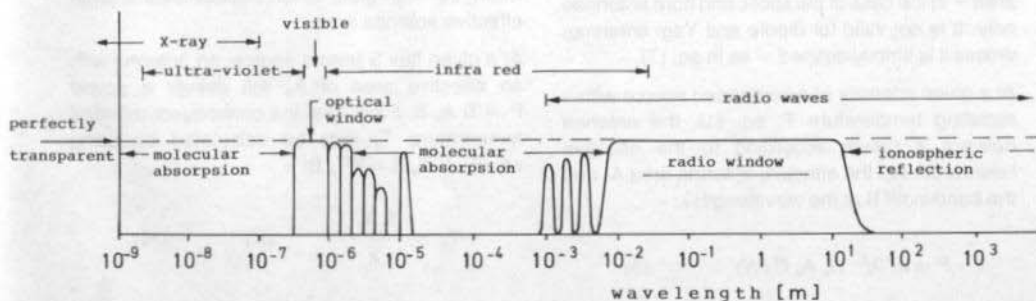


Fig. 3: The total transparency of troposphere and ionosphere



shorter wavelengths within this window. Another effect is that the signal is deflected and appears to originate from a point higher in the heavens than is actually the case.

In the mm-wavelength band there is another region of low attenuation between the O₂ and the H₂O absorption bands. Below 0.3 mm, however, the atmosphere is absolutely impervious and remains so until the vicinity of the infra-red region corresponding to a few μm , as can be seen in fig. 3.

4. ANTENNAS

The most prominent feature of an antenna is its directional characteristic. This determines the spatial resolution properties by which the heavens may be explored. The angular displacement Θ between the maximum and the half-power point on an antenna's polar diagram, is determined by the relationship between the wavelength λ to the paraboloid's diameter D and may be given approximately by: -

$$\Theta = 60 \lambda/D \text{ (degrees)} \quad (2)$$

The sensitivity of the antenna as a radiation receiver is described by the effective area of the mirror A_e . This extraordinarily helpful quantity has a direct relationship with the geometrical antenna area - in the case of parabolic and horn antennas only. It is not valid for dipole and Yagi antennas unless it is strictly defined - as in eq. (7).

At a given intensity of an extended source with a radiating temperature T , eq. (1), the antenna delivers a power according to the effective beamwidth Ω_e , the effective antenna area A_e and the bandwidth B at the wavelength λ : -

$$P = kT/\lambda^2 \cdot \Omega_e A_e B \text{ (W)} \quad (3)$$

The antenna's effective beamwidth Ω_e is expressed in terms of the beamwidths in both the

E-plane $\Delta\Theta$ and the H-plane $\Delta\Phi$ and is given by: -

$$\Omega_e = 4.1 \times 10^{-4} \Delta\Theta \Delta\Phi \text{ (rad.)}$$

$$\lambda^2 = A_e \Omega_e \text{ (m}^2\text{)} \quad (4)$$

Therefore eq. 3 can be simplified to: -

$$P = kTB \text{ (W)} \quad (5)$$

An antenna which is "illuminated" by a black body of temperature T and bandwidth B , delivers at its output terminals a power kTB . This power is identical with the noise performance of a resistance which has a temperature T . This fact is used for the absolute calibration of the radiometer system.

A receiver which has been calibrated by this means measures just about the same input power in Kelvin antenna temperature. This has nothing at all to do with the ambient temperature which the antenna is subjected to. It is that temperature which a black body must have to produce the same power at the antenna output terminals. The antenna temperature, when fully illuminated, is then identical with that of the radiator's. In this case, a simple dipole will deliver the same power as a high-gain antenna but, of course, this cannot possibly be the case. Actually, the antenna temperature becomes smaller as the relationship between the antenna beamwidth and the source diminishes (7).

An observation of a source having very small dimensions requires an antenna of low beamwidth, i.e. high gain, which necessitates a large effective antenna area.

At a given flux S from a source, an antenna with an effective area of A_e will deliver a power $P = S A_e B$. From this, the consequent antenna temperature T_a may be calculated by using eq. (5): $S A_e B = k T_a B$: -

$$T_a = \frac{S A_e}{k} \text{ (K)} \quad (6)$$

The strongest sources, Cassiopeia A and Cygnus A have a flux of some 10,000 Jy. Even with an

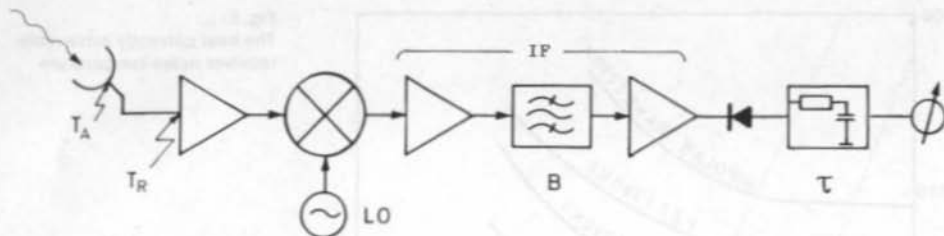


Fig. 4: Block diagram of a typical radiometer

antenna of effective area of only 1.5 m^2 results in an antenna temperature of approximately 10 K. This knowledge, on the face of it, seems to imply little difficulty, but nothing has been mentioned about the effect of interference in the observation frequency band.

EME experiments by radio amateurs give some idea of what the antenna requirements have to be for astronomical purposes. At least the same antenna system as used for amateur astronomy as is used for amateur EME communication: parabolic dishes up to six metres diameter i.e. an effective antenna area of 20 m^2 or a Yagi array with 20 to 24 dB gain would be ideal. The effective antenna area may be arrived at for a Yagi array in the following manner: The gain G is defined from the relationship $G = 4\pi/\Omega_e$, where the gain G is referred to an isotropic radiator. The effective antenna area is then given by: -

$$A_e = \frac{G \lambda^2}{4\pi} \quad (\text{m}^2) \quad (7)$$

An antenna having a gain of 23 dB (200) has an effective antenna area of $A_e = 7.8 \text{ m}^2$ in the 70 cm band.

5. RECEIVER

The most important component part of a radio-astronomy installation is the receiver. Super-

heterodyne receivers, familiar to all radio amateurs, are invariably employed (2, 4, 5, 6, 7). The block diagram of fig. 4 shows such a receiver. In the place of the demodulator a quadratic detector has been employed. This gives a voltage output which is proportional to the noise power input to the receiver (8). The noise power is directly proportional to the bandwidth B of the IF amplifier. An integrating network follows the detector which has a time constant τ . This introduces a time average into the noise power. The averaged signal is then further amplified and taken to a pen recorder.

The noise temperature of the whole system is T_r . The noise power referred to the receiver input is $P_r = k T_r B$. The bandwidth B should be as large as possible for the observation of continuous sources and consequently the signal power, in accordance with eq. 5, will be accordingly large. An IF bandwidth will be a few MHz wide in the metric bands and up to 100 MHz in the centimetre bands. Assuming that $B = 10 \text{ MHz}$ and $T_r = 100 \text{ K}$, then the total power at the receiver input terminals will be:

$$P_r = k T_r B = 1.4 \times 10^{-14} \text{ W},$$

i.e. - 109 dBm approx.

This will be amplified in the receiver to approximately 10^{-5} W , i.e. - 20 dBm approx. at the detector diode. This results in a total voltage gain G_v for the receiver of 90 to 100 dB from antenna input terminals to detector.

An automatic gain control is not fitted to the receiver as the signals under examination are of the same order as the receiving-system's own internally generated noise.

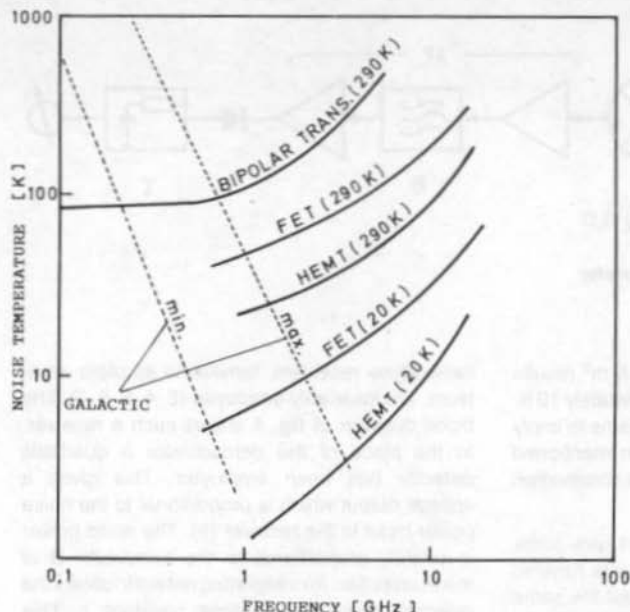


Fig. 5:
The best currently achievable
receiver noise-temperature

The wanted cosmic signals are fed, together with the indistinguishable system noise, to the receiver input and having a total power of P_s , which stems from the antenna temperature T_a . The total power consisting of the sum of the noise power and the signal power present at the detector diode is then: -

$$P = G_v k B (T_r + T_a) \quad (W) \quad (8)$$

Normally T_a is noticeable smaller than T_r . The object then is to identify a signal which has been buried in the receiver system noise.

Radio communication techniques can normally rely upon the received signal being many times as strong as the average receiver-system noise power. This would be in accordance with the comparison of P_s and P_r in the above case, if the absolute value in the average receiver-system noise power in the astronomical case is not considered, but only their variations. This is why it is meaningful, as the average value of the noise power can be measured and compensated for by the time constant τ of the detector integrator network. The actual unwanted noise are the

variations which this DC output signal has impressed upon it. Their magnitude depends, of course, upon the time constant τ but also upon T_r and the IF bandwidth B . The relationship gives rise to the formula given by Dicke which gives the RMS value of the variations T_{min} : -

$$T_{min} = \frac{T_r}{\sqrt{B \tau}} \quad (K) \quad (9)$$

For example; if $\tau = 10$ s, $B = 5$ MHz, $T_r = 100$ K then $T_{min} = 0.014$ K. This means that an antenna temperature $T_a = T_{min}$ can be measured with a signal-to-noise ratio of unity!

For example, say if under these conditions a source having a T_a of 5 K is under observation. The ratio $S/R = 354$, i.e. when the antenna is directed to this source, the receiver output voltage, the RMS value of the receiver produced system noise, rises by a factor of 354.

In order that the receiver sensitivity can be as large as possible, the IF bandwidth and the

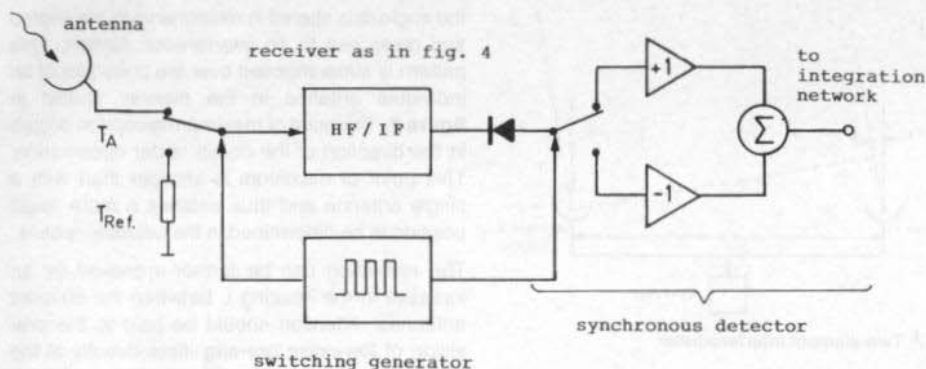


Fig. 6: "Dicke-switch" radiometer

integration time must be as large as possible in accordance with eq. (9). This then ensures that the receiver noise temperature is as small as possible. The methods of ensuring this are familiar to radio amateurs, noise temperatures under 100 K are able to be achieved well into the GHz range by means of GaAs-FET pre-amplifiers.

Unfortunately, the limit sensitivity as indicated by eq. (9) cannot quite be achieved. The cause of this lies in the inconsistency of the overall amplification due to the temperature variations, supply voltage fluctuations and receiver intrinsic noise. In particular, the low-frequency $1/f$ -component of the total noise, which originates in the active components together with DC drift in the amplification following the integration network, are responsible for a large part of the short-fall in performance.

In 1946, Dicke developed a receiver which went a long way to eliminating these defects. The block diagram is shown in fig. 6. This type of receiver switches the receiver input between the antenna and a constant-temperature termination resistor $R_{ref.}$ at a rate of 10 to 100 Hz. In a synchro-detector, the detector output voltages are separated from each other and the two components. Two quantities are measured: receiver noise + antenna signal and then, receiver noise + reference signal. Then they are subtracted from each other. The termination resistor produces

the noise power $kT_{ref.}B$. The periodic output signal has an amplitude: -

$$U_{pp} = \eta G_v k (T_a - T_{ref.}) (V) \quad (10)$$

where η is the diode sensitivity given in V/W.

It can be shown that the gain variations are nullified when T_a is arranged to be equal to $T_{ref.}$.

Even when this calibration is disturbed due to temperature variations in the reference termination, the "Dicke switch" has the advantage of suppressing the DC component to the level of the receiver basic noise. This facilitates linear amplification in the final DC amplifier thereby reducing the $1/f$ component to zero.

6. INTERFEROMETER

The resolution of a radio telescope can be dramatically improved by employing the interferometer principle. This principle offers the amateur one of the greatest possibilities to improve the system at a low-capital outlay.

The simplest interferometer consists of two identical antennas separated by a distance L in the east-west plane (fig. 7). The greatest antenna gain is perpendicular to this plane. The elevation

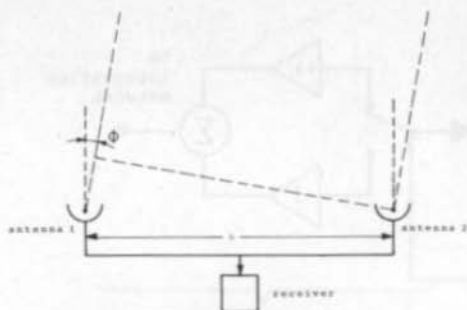


Fig. 7: Two-element interferometer

is so adjusted that the antenna is directed to the source when the latter is in the meridian. The signals from the source are fed to the receiver by two transmission lines of equal length.

A signal arriving at an angle Φ to the plane of the antenna will produce two components with a phase difference of $(\pi L/\lambda) (\sin \Phi)$, where λ is the wavelength at the working frequency. The components at the detector outputs will have an identical phase difference and will add vectorially to produce a voltage U . This is related to the incidence angle Φ by: -

$$U = (1 + \cos (2\pi L/\lambda \times \sin \Phi)) \quad (11)$$

If, owing to diurnal movements, the object under observation passes through the antenna lobe,

the angle Φ is altered in relationship to the source and gives rise to an interference pattern. This pattern is superimposed over the polar plot of an individual antenna in the manner shown in figure 8. The point of maximum reception occurs in the direction of the object under observation. This point of maximum is sharper than with a single antenna and thus enables a more exact position to be determined in the celestial sphere.

The resolution can be further improved by an increase in the spacing L between the element antennas. Attention should be paid to the provision of low-noise pre-amplifiers directly at the antenna terminals in order to mitigate the increased loss caused by the longer transmission lines. Both pre-amplifiers should have constant group-delays and be identical in all other respects.

The two-element interferometer can be usefully modulated at periodic points in the antenna transmission lines. This is injected by means of a $\lambda/2$ line to one antenna, and the modulation also synchronously demodulates the receiver output. The synchrodyne demodulation has the effect of subtracting the elemental patterns of fig. 8, one of which has been delayed by the $\lambda/2$ line. The result is that the subtraction yields a minimum in the middle where there was formerly a maximum.

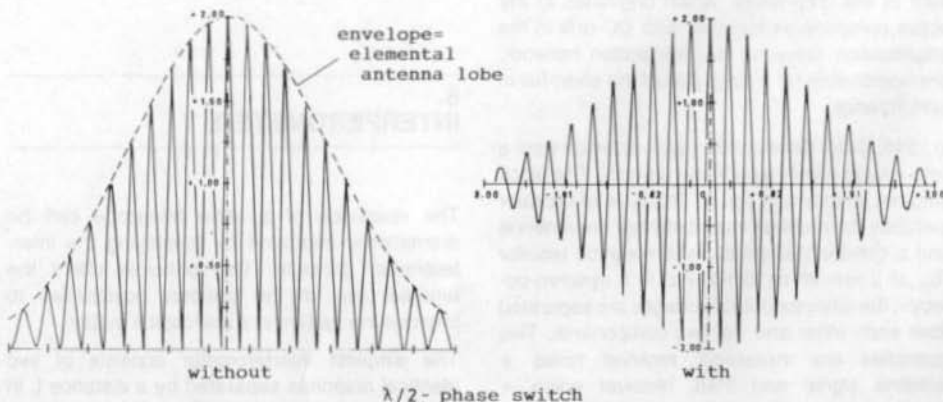


Fig. 8: Two-element interferometer interference pattern



From the foregoing, it will be quite apparent that there will be no great challenges presented to the amateur by the construction of an interferometer. All it requires is, for example, two Yagi arrays comprising 2 to 4 elemental antennas each with 10 dB_a gain, and spaced by a distance of 10 metres. This installation will be sufficient to examine the stronger astronomical radio sources (10).

7. CELESTIAL OBJECTS

The Sun is the strongest source in the whole cosmic radio spectrum (9). Its radiation can largely be separated into four types: the Sun's quiescent radiation, the slowly varying Sun-spot component, the noise storms in the metre-wave range and the large outbreaks of radiation. Above 10 GHz and under 100 MHz the Sun behaves as a black-body radiator. Outbreaks of radiation are largely confined to the metric bands and can increase the Sun's flux by as much as an order, fig. 2.

The radiation from a planet is mainly thermal in nature and in accordance with its surface temperature, about 500 K for the nearest planet to the Sun, Mercury, and approximately 50 K for the outer planets, Neptune, Uranus and Pluto. In the metric-wave region, they are therefore the very weakest of radiators. They only become strong sources in the mm-wave region in accordance with eq. (1).

The same applies to the Moon. Its radiation is shown in fig. 2. The Moon is a prime example of a

thermal radiator. Its mean temperature amounts to some 230 K and superimposed upon this are the periodical extremes caused by the Moon's phases. These relationships are so well-known that the Moon can be employed as a system calibration source.

Only the planet Jupiter deviates clearly from a thermal radiator. Its intensive radiation outbreaks in the short-wave range were eluate known in 1955, again, purely by chance. The surface temperature is 130 K in accordance with the radiation temperature measured in the 3 cm waveband. In the 10 cm band, the radiation temperature amounts to approximately 600 K and at 70 cm above 50,000 K. The cause of this evident non-thermic emission is the gyrating movement of fast electrons in the magnetic field of Jupiter. The observed intensive radiation is then a synchrotron radiation.

Table 1 lists the strongest radio sources, after that of the Sun, in the 200 MHz region:

Of the galactic objects, the remnants of supernovae are mainly the stronger radio radiators. The best known is the Crab Nebulae, the name of this source is Taurus A. Another one is Cassiopeia A, the strongest radio source, apart from the Sun, that can be detected upon Earth.

The second strongest radio source is Cygnus A, a galaxy 550 million light-years away. The intensity with which this source emits radio waves is enormous. It exceeds its light emission by many times in power output. Objects possessing these characteristics are known as radio galaxies. Cygnus A is the most prominent representative of over 100 so far known objects of this kind.

Name	Flux (Jy) (200 MHz)	Type
Cassiopeia A	11000	Super-novae remnant
Cygnus A	8100	Galactic
Taurus A (Crab Neb.)	1400	Super-novae remnant
Virgo A	970	Galactic
Sagittarius A	1000	Galactical core

Table 1



8. REFERENCES

- (1) J. S. Hey: Das Radiouniversum, Verlag Chemie, Weinheim (1974)
- (2) J. D. Kraus: Radio-Astronomy, McGraw-Hill, New York (1966)
- (3) C. A. Muller: Ein Empfänger für die Radiostrahlung des Wasserstoffs Philips Techn. Rundschau, 10, 317 (1956) und 11, 361 (1956)
- (4) O. Hachenberg, B. Vowinkel: Technische Grundlagen der Radioastronomie, Bibliographisches Institut, Mannheim (1982)
- (5) Kristen Rohlf's: Tools of Radioastronomy, Springer-Verlag, Berlin (1986)
- (6) G. Hoch: Determining the Sensitivity of Receive Systems with the Aid of Solar Noise.
- VHF COMMUNICATIONS Vol. 12, 1980 Ed. 2, P. 66 - 72
- (7) D. Dobričić: Determining the Parameters of a Receive System in Conjunction with Cosmic Radio Sources. VHF COMMUNICATIONS Vol. 16, 1984 Ed. 1, P. 35 - 50
- (8) C. Vieland: 50 Ω Wideband Detectors VHF COMMUNICATIONS Vol. 20, 1988 Ed. 2, P. 111 - 125
- (9) W. Altenhoff: Radioastronomie für Amateurastronomen, Handbuch für Sternfreunde, 3. Auflage, Springer-Verlag, Berlin (1986)
- (10) G. W. Swenson: An Amateur Radio Telescope Sky and Telescope, 55, 386 (1978)
55, 475 (1978)
55, 28 (1978)
56, 114 (1978)

A very detailed and comprehensive

AMATEUR RADIO PROGRAM

for the **ATARI ST**

de DK4BV ©

- Terminal program for packet radio and AMTOR
- RTTY program
- Amateur logbook
- Contest operation
- Antenna headings and distance calculations
- Determines moon and satellite positions
- CW trainer and much more!

Description in VHF Communication 3/89.



Program diskette in English
(version 10.5x)

Art.No.: 3403/9.x **DM 190.00**

Please give callsign and QTH
location code when ordering!



Telecommunications, VHF-Communications - UKW-Technik Terry D. Bittan
Jahnstraße 14, D-8523 Baiersdorf, Telefon (091 33) 470, Telex 629887



Peter Gerber, HB 9 BNI

Calculating the Sun and Moon's Kepler Elements

Radio communication via satellite working has increased steadily over the last few years. Also, the equipment in ground stations has improved. Many satellite stations are now coming to the point where they are able to make EME contacts with the larger EME stations (1). Now, many radio amateurs wish to test the efficacy of their stations by using the sun's noise radiation as a measurement source (2,3.) This fact led to the desire to be able to calculate the position of both the sun and the moon by means of available satellite-orbit, computer programs.

Some of these programs do give, at least, the position of the sun but simpler programs do not even go this far. The main cry is always for the provision of the "Kepler Elements" for the sun and the moon. This short article will attempt to show how far this desire can be fulfilled and how the Kepler Elements may be calculated.

The following explanation will use terms and expressions which have been drawn from astronomy and from the field of satellite technology. A good explanation of this may be found in (4).

1. THEORETICAL CONSIDERATIONS

In principle, it is not possible to give Kepler Elements for the sun or the moon for the following reason: -

When Kepler Elements for a satellite are given, it is automatically assumed that the satellite is moving in the immediate gravitational field of the earth and is influenced by no other body (i.e. from the sun or moon). The known mass of the earth determines the relationship of the large half-axis of the satellite's orbit and the orbital time (and thereby the "Mean Motion"). See the formula in (5). This dependence is calculated in every satellite program and cannot be changed by introducing orbital elements. In addition, the co-ordinate system used is based upon the middle point of the earth which also cannot be altered. The inclination of the orbit - that is, the angle of the plane of the orbit has with that of the equator - is taken as being a constant and also cannot be altered by the program.



1.1. Sun

The sun's movements are not in the least affected by the earth owing to the enormous disparity between their respective masses. Most sun-calculating computer programs are tending nowadays to calculate the orbit in a co-ordinate system which is centered on the middle point of the sun. Also, owing to the huge mass of the sun, the relationship between orbital time and the large half-axis is somewhat different.

It is possible, by means of a co-ordinate transformation, to consider the earth to be in a fixed position and allow the sun to move. This would result in a "sun's orbit" having a transit time of one year. The plane of the orbit inclined relative to the earth's equatorial plane, would be 23.44° . The problem of the varying distances cannot, however, be transformed away. The large half-axis (radius) of the sun's orbit amounts to some 152 million kilometers. The satellite program provides for a transit time of one year but an orbit half-axis of only 2.16 million kilometers. Both distances, actual and given, are extremely large compared with the earth's diameter making the error in both azimuth and elevation very small.

Any path-loss attenuation given by the program will, of course, be wrong.

The Kepler Elements may indeed be given for the sun but the correct distance calculation will have to be dispensed with.

1.2. The Moon

In the case of the moon, the problem of distance is not so marked. The radius of the moon's orbit is about 406,700 km and the satellite program yields, for a transit time of 27.32166 days, an orbit radius of 383,169 km. Using a calculated azimuth and elevation would indicate an error of 0.05° which can, of course, be neglected. On the other hand, the path-loss computation will be noticeably in error.

The main problem with calculating the moon's orbit is that the inclination of the orbit is not constant. The plane of the moon's orbit is inclined 5.15° to the ecliptic (the plane of the earth's orbit around the sun). The ecliptic, in turn, is 23.44° inclined to the equatorial plane of the earth. The satellite program is looking for a result of an inclination based upon that of the equatorial plane. This inclination varies according to how these three planes are disposed to each other at the time. It fluctuates, at its greatest extent, to 28.6° ($23.44^\circ + 5.15^\circ$), to a minimum of 18.3° ($23.44^\circ - 5.15^\circ$). How this apparent inclination varies over a period of 8000 days may be extracted from **fig. 1**. The inclination follows roughly a cosine law having an average value of 23.44° .

Perhaps it may now be apparent how high the moon has appeared in its trajectory over the last few years. The highest moon in the sky occurred on 21st November 1987 when the inclination was at its greatest. A good nine years later, the minimum height will be achieved when the moon will be some 10° lower. That is the equivalent of twenty full-moon diameters lower!

There is, however, a further problem concerning the moon. The program calculates a satellite's orbit from the Kepler data and the earth's mass and arrives at a value for the apsis anti-node and node transition points. (The programs from Meinzer (6) require these quantities to be inserted as V and Q.) Also, the moon's orbit exhibits both an apsis anti-node and a node transition but these perturbations are caused much more by the sun than by the earth. The satellite program therefore computes these quantities falsely from the Kepler Elements and after a time, the

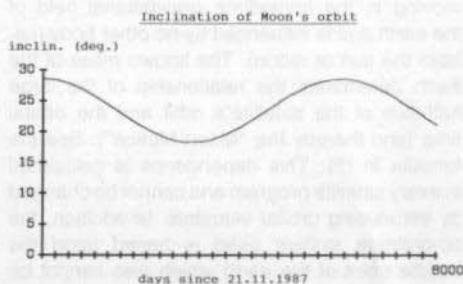


Fig. 1: Change in the inclination of the moon's orbit for the next 8000 days.
X-axis graduations = 300 days



orbit calculation is in error. The apsis-line (interconnecting line from perigee to apogee) turns with a period of 3232 days in a clock-wise direction. The node-line (interconnect-line between ascending and descending nodes) revolves with a period of 6798 days. This results in the following correction factors: –

Nodal point:
dRAAN/day (Q) = $-0.052953^\circ/\text{day}$

Apsis anti-nodal point:
dAPOG/day (V) = $0.111399^\circ/\text{day}$

The program calculates these quantities from the given Kepler-Elements (eccentricity inclination) and the earth's mass and results (for the maximum possible inclination of 28.6°) in the following:

Nodal point:
dRAAN/day (Q) = $(-5.192752 \times 10^{-6})^\circ/\text{day}$

Apsis anti-nodal point:
dAPOG/day (V) = $(8.471243 \times 10^{-6})^\circ/\text{day}$

In the more modern programs, these correction factors cannot be altered manually and the moon's orbit, after 200 to 300 days, will be computed significantly in error. This error, after 200 days for an ascending node, amounts to 10.5 degrees and the same for the argument of the perigee is 22.2 degrees.

Furthermore, the moon's orbit is not a perfect ellipse (as the satellite program assumes!) but is in fact distorted by the gravitational field of the sun and to the attractions of other large planets as well. An exact moon orbit calculation must take into account several hundred of these perturbing influences. The Kepler Elements cannot allow these perturbations to be included.

For these reasons, it is only possible to give the moon the so-called osculatory elements (Latin osculus: kiss). That means, the calculated orbit follows the actual orbit for a while but the orbits then depart far from each other. The time span over which the computation is required determines its accuracy. For example, a tolerated departure of up to 10 degrees in the moon's calculated orbit as opposed to its actual orbit can be simulated for about one year.

2. PRACTICAL APPLICATION

2.1. Sun

The following fixed data of the sun's orbit (4.7) is the starting point:

Eccentricity	0.01672
Inclination	23.44°
Decay rate	0
MM (tropics)	0.002737909256 corresponding to a tropical transit of 365.24220 days

A genuine sun program will now be able to determine the exact point of the ascending node time. This occurs on 21st March of any year. The right ascension of this point is, by definition, zero. This time is known as the epoch. The mean anomaly of the sun at this time is known as the MA. The geocentric ecliptical length at this time has also to be computed.

All that is missing now is the perigee's argument, that is, the angle must be covered until the next perigee is due. This lies at the beginning of January. It is to be found as the point in time with mean anomaly = zero or at minimum distance. To be calculated is the geocentric ecliptical length at this time. The difference to the corresponding epoch's quantity reveals the argument of the perigee. With that, all elements are known.

2.2. Moon

The following fixed data of the moon's orbit is the starting point (4, 7): –

Eccentricity	0.0549
Decay rate	0
MM (sidereal)	0.036600996, corresponding to an average orbital time of 27 days, 7 hours, 43 mins, 11.5 seconds.

A genuine moon-orbit program would now search for the time of an ascending node in the vicinity of the desired epoch. This is the moment when the geocentric declination changes from minus to plus. The right ascension to this point



in time is the right ascension of the ascending node, the time is the epoch.

Now the inclination to this time (or better, about 150 days later) must be determined. A point in time of 150 days later will in fact be chosen in order that any error arising will be spread. Otherwise, the satellite program will compute the data directly after epoch correctly but would then relatively quickly start making bigger errors. This is the way in which the errors are distributed, first in the vicinity of the epoch then they become smaller and later become gradually larger. The data can then be used over a longer period.

The inclination is calculated as follows: -

$$23.44^\circ + 5.15^\circ \cos ((\text{days since } 21.11.1987 / 6798) 360^\circ)$$

An exact computation cannot be expected as no disturbing influences have been taken into account but it is still a good calculated estimate.

Now, the next thing is to search for the forthcoming perigee, i.e. the time when the mean anomaly is zero. The difference of the geocentric ecliptical length between the epoch and this point in time is the argument of the perigee. In order to be absolutely correct, the difference of the true anomaly must be determined and this is very often not known. As the ecliptic relative to the plane of the moon's orbit is only 5° , the error remains small and can be neglected in comparison with the other inaccuracies. With this, all elements are known.

3. KEPLER ELEMENTS FOR MID-1989

Following the methods given previously, the two Ephemeridian data for sun and moon were calculated. The series corresponds to the NASA "two-line elements".

Sun:

Year of epoch	1989
Day of epoch	79.63819444 = 20.3.1989 15 h 19 m

Change in mean motion	0
Inclination	23.44°
RAAN	0°
Eccentricity	0.01672
Argument of perigee	282.77°
Mean anomaly	75.38°
Mean motion	0.002737909256
Current epoch number	1989

Moon:

Year of epoch	1989
Day of epoch	176.65916667 = 25.6.1989, 15 h, 49.2 m
Change in mean motion	0
Inclination	27.5° (for the 25.6.1989: 27.86°)
RAAN	354.05°
Eccentricity	0.0549
Argument of perigee	20.20°
Mean anomaly	341.343°
Mean motion	0.036600996
Current No. of epoch	as desired

4. COMPARISON

The positions of the sun and moon calculated by using the above Kepler Elements are compared with their actual positions by means of a specially designed program. A satellite program by HB 9 BNI together with a sun and moon program from the same source, was employed for this purpose. This program was devised in the TURBO PASCAL V4.0 computer language. All the calculations were based upon HB 9 BNI's QTH and the computer in use was an IBM-compatible PC with co-processor. The data was also controlled with the GRAPHTRAK SILICON EPHEMERIS the results of which agreed very closely with the data derived from HB 9 BNI's program. Thanks are expressed to M Forrer HB 9 BMN for the work involved in this process.

**Sun:**

All calculations for
12.00 UT, angles are in
degrees

Date	Sat program		Sun/Moon-prgm		Error deg.
	AZ	EL	AZ	EL	
15. 8.1989	191.88	56.33	191.47	56.46	0.26
15.11.1989	192.10	23.38	191.85	23.58	0.30
15. 2.1990	184.86	30.00	184.59	30.16	0.28
15. 5.1990	197.26	60.83	196.81	60.95	0.25
15. 5.1991	197.24	60.77	196.78	60.90	0.26
15. 5.2000	197.32	60.96	196.86	61.09	0.26
15. 5.2089	197.36	61.06	196.84	61.20	0.29

Moon:

Date	Time UT	Sat program		Sun/Moon prgm		Error deg.
		AZ	EL	AZ	EL	
15. 8.89	23.00	188.12	21.48	186.91	21.75	1.16
15.11.89	01.00	181.73	69.88	181.48	69.92	0.09
15. 2.90	03.00	176.31	28.78	173.81	26.79	2.97
15. 5.90	04.00	185.30	17.79	185.23	18.95	1.16
15. 8.90	07.00	178.59	69.91	191.17	68.95	4.51
15.11.90	09.00	175.15	28.57	169.68	25.10	5.99
15. 2.91	12.00	174.47	33.51	176.15	35.50	2.41
15. 5.91	13.00	175.45	69.98	190.76	67.70	5.96
15. 8.91	15.00	174.00	28.33	165.81	23.37	8.88

The moon-data table and **fig. 2** show that the error remained under 6° for more than one year following the epoch. Then, the error began to climb rapidly. Since the half-power points of a typical satellite antenna lie over 10° , this error is entirely tolerable for initial experiments or for noise measurements of the sun (less than 0.3° error).

4.1. Conclusions

Theoretically, it is not possible to give Kepler Elements for either the sun or the moon in order that they may be used, together with a satellite program, to calculate the exact position of these bodies. If, however the calculation for distance is dispensed with and also deviations up to 8° can be tolerated, the calculations using Kepler Elements are entirely feasible. The achievable accuracy is approximately 0.25° for the sun over the next 100 years and about $6 - 8^\circ$ for the moon lasting for one year following the

epoch. As amateur accuracy demands for antenna measurements and EME experiments are not likely to be higher, these elements can be regarded as a usable substitute for a specialized program.

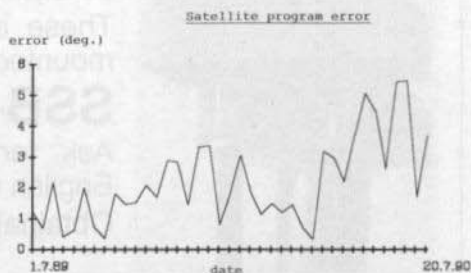


Fig. 2: Representation of the angle difference (degrees) between the moon's true position and the mean of its position as calculated using Kepler Elements, for one year after the epoch. Each division on the X-axis is 10 days.



5. REFERENCES

- (1) Gerber P., HB 9 BNI:
EME für jedermann
Old Man 9/1986, p. 23 - 26
- (2) Hoch G., DL 6 WU:
Determining the Sensitivity of Receive
Systems with the Aid of Solar Noise.
VHF COMMUNICATIONS 12 (1980), ed. 1,
p. 66 - 72
- (3) Lund D., WA 0 IQN:
Using Sun Noise
QST April 1968, p. 42 - 43
- (4) Herrmann J.: DTV-Atlas zur Astronomie.
München 1974
- (5) Bohrmann A.:
Bahnen künstlicher Satelliten,
BI Hochschultaschenbücher;
Mannheim, 1966
- (6) Meinzer K., DJ 4 ZC: Klein aber fein.
AMSAT-JOURNAL 15, February 1984
- (7) Schaifers K., Traving G. (Hrsg.):
Meyer's Handbuch über das Weltall.
Mannheim, 1973.



MICRO-AMP with VOX/PTT

Low-noise GaAs-FET pre-amplifiers with outstanding features and favourable prices

2-m model MC-2 **DM 249.50**

70-cm model MC-70 **DM 259.00**

These are two of the low-noise mast-mounted pre-amplifiers of the

SSB-Electronic series

Ask for the Shortform Catalogue in English (free of charge)

Obtainable for original prices from:



Joachim Berns, DL 1 YBL

24 / 23 cm-Band Linear Power Amplifier Module M 57762

The linear final amplifier described in this article consists of two Mitsubishi M 57762 hybrid amplifiers, in RF isolation from each other, feeding the common output. A one-module version will also be described which may either be used "bare-foot" or as a PA driver stage.

In particular, the parallel PA stage is characterized by its simplicity and unproblematical drive requirements. The construction requires no special PCB materials, such as PTFE, and also no special components. It can, in fact, be constructed, as soon as the two M 57762 modules have been obtained, from materials available from most radio amateur workshops.

1. SINGLE-MODULE PA

A single-module stage will be described first as this is the basic module which can be used to drive the double-module PA (formed also from the same circuits). See figures 1 to 4.

A proprietary tin-plate box dimensioned 37 x 74 x 50 mm is used to house the module. No cut-outs should be provided in the cover for the module as unfavourable earth connections could be formed, which could encourage oscillations, thus diminishing the output power. The lower cover of the tin-plate box should be soldered

completely around its perimeter, to the walls of the box, in order to achieve a good electrical and mechanical contact. The ground tabs of the hybrid module are secured with two M4 screws to the enclosure cover and the heat sink fitted.

The supply voltage is introduced via feed-through capacitors. The capacitors C1 comprise small 5 x 5 mm (approx.) pieces of two-sided PCB material which serve as HF terminal points as well as a decoupling capacitor. They are soldered directly to the bottom cover of the enclosure. The capacitors marked C are made from a combination of 1 nF ceramic plate capacitors soldered to the bottom cover directly under the module connections 2, 3 and 4, and a 4.7 nF and 10 μ F tantalum capacitor.

For AM-ATV and SSB working, C2 and C3 (tantalum capacitors) should also be added to the

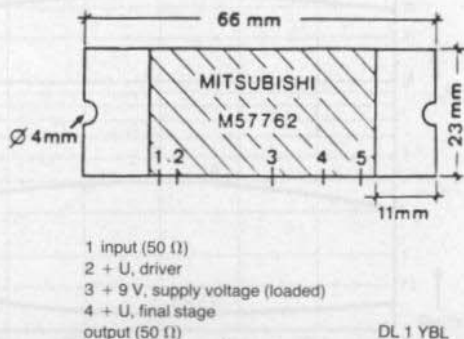


Fig. 1: Module dimensions

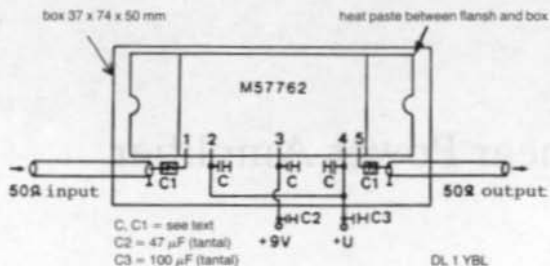


Fig. 2: Wiring diagram

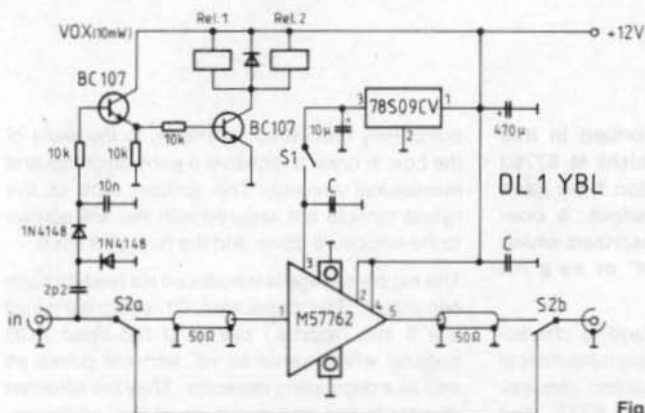
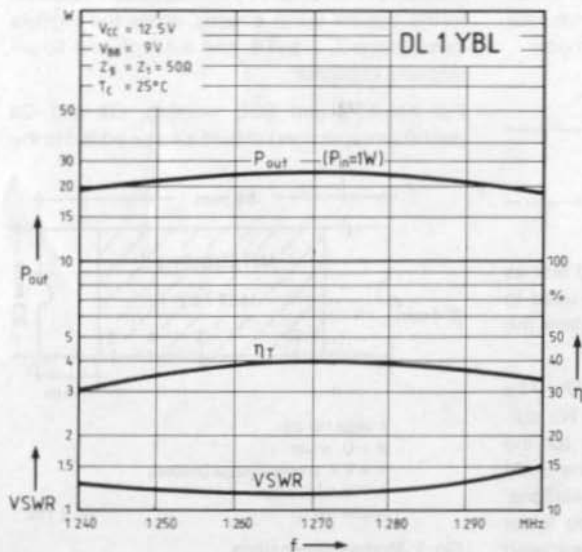


Fig. 3: Single-module PA with HF VOX

Fig. 4: Output power P_{out} , efficiency η_T , input VSWR as a function of frequency

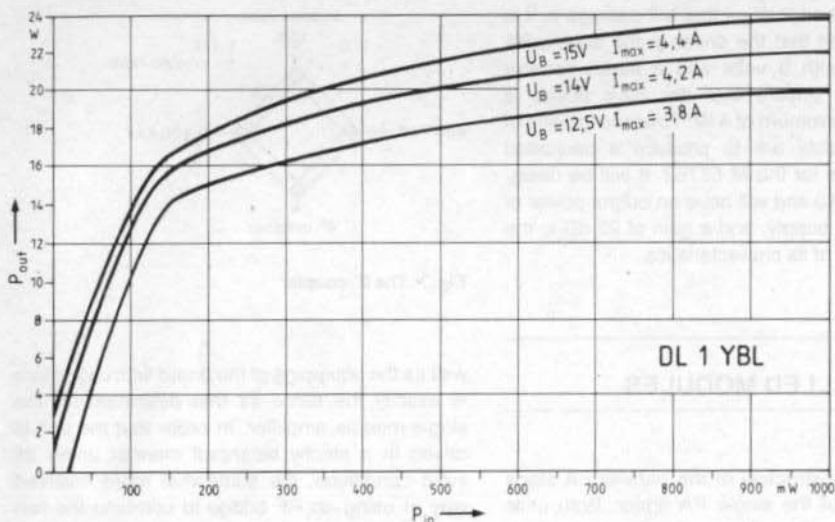


Fig. 5: Characteristic of a MM 57762 single-module amplifier (freq. = 1260 MHz)

de-coupling. The input and output matching is so good that the usual series preset capacitor used for this purpose may be dispensed with.

1.1. Power Characteristics

The data of the power amplifier, which was constructed in accordance with the information given here, is shown in fig. 5. It may be seen that

the maximum peak input driving power for SSB working is 200 mW. The maximum amplification in the linear region and at 14 volts supply, is approximately 20 dB. If the amplifier is required for FM-ATV etc. it can be run into the saturation region with a power output up to 22 W without any fear of any ratings being exceeded.

When using this module as a driver for a double PA, it is to be ensured that the input drive power

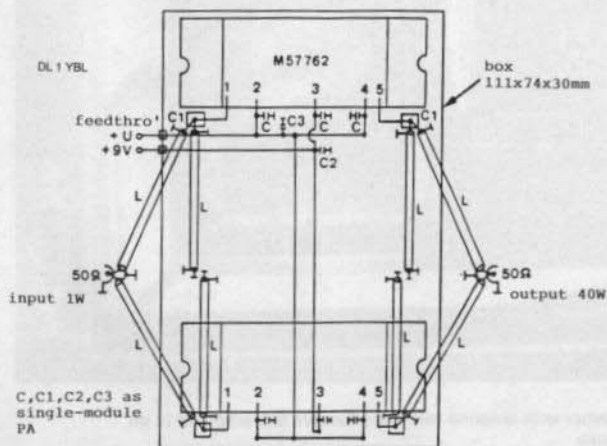


Fig. 6: Parallel final amplifier



does not exceed 2 W as this will damage it. It is for this reason that the driver in the double PA is supplied with 9 volts and a series resistor employed to ensure that the drive power is limited to a maximum of 4 W. Towards the end of 1988, Mitsubishi are to produce a dedicated driver module for the M 57762. It will be designated M 67715 and will have an output power of 2 W at 7.2 V supply, and a gain of 22 dB in the linear portion of its characteristics.

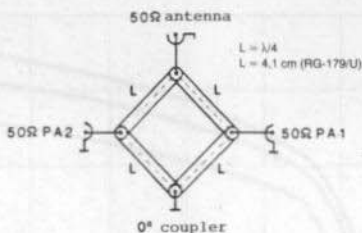


Fig. 7: The 0°-coupler

2. PARALLELED MODULES

The basic construction of the parallel PA stage follows that of the single PA driver. Both units are housed in the proprietary box 111 x 74 x 30 mm (fig. 6). The wiring of the supply voltage as

well as the equipping of the board with capacitors is exactly the same as that described for the single-module amplifier. In order that the unit is driven in a strictly balanced manner under all input conditions, the somewhat more involved way of using an RF bridge to combine the two module elements was employed. The so-called 0°-coupler (fig. 7) offers a very simple con-

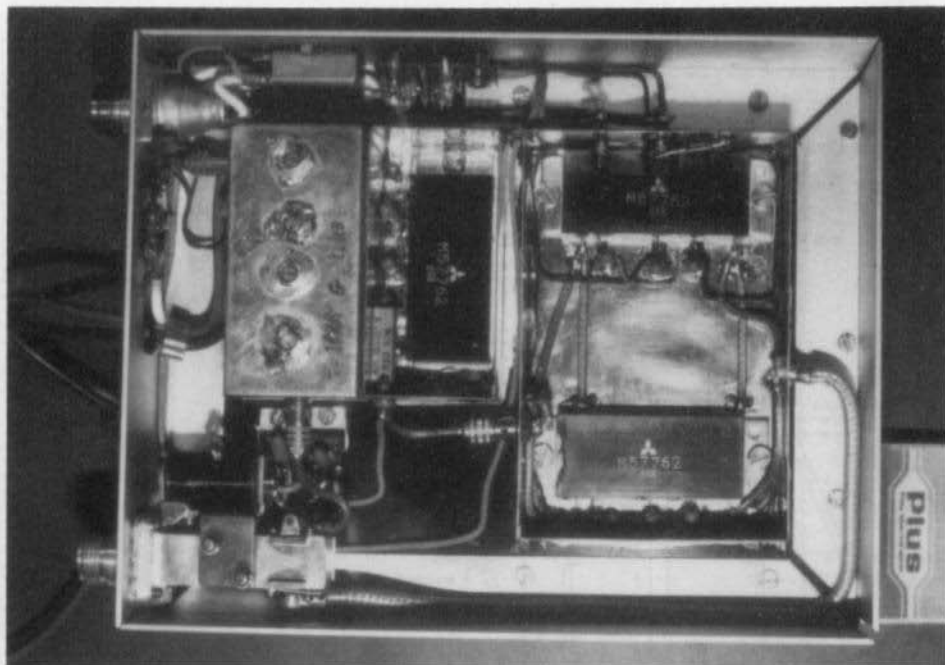


Fig. 8: Both the described amplifiers together with antenna relay and receive pre-amplifier in an aluminium frame on a large heat-sink



struction with sufficient isolation between the two branch amplifiers PA 1 and PA 2, for amateur purposes. The transformation is effected by means of four $\lambda/4$ lengths of 75 Ω cable (RG-179/U or similar). The author used 4.1 cm lengths of thin PTFE cable which are soldered directly on to the tin-plate box.

Under no account should ordinary wire be employed for this purpose as spurious oscillations are sure to occur.

2.1. Performance Data for the Double PA

The double PA constructed by the author required 2 W input power to drive it to 40 (or 48 W as required) at a supply voltage of 14 volts.

The efficiency is not particularly high, all examples having, however, more than 30 % efficiency. With a power output of 40 W and a DC supply power of 120 W, a large heat-sink must be employed. The big advantage of this PA stage is that it covers the whole of the 24 cm band without tuning being required and with no need to adjust the drive.

The unit is very robust and will withstand a VSWR of 16 : 1 at full output power. The maximum supply voltage is 17 volts and the second harmonic suppression is 30 dB, the third harmonic suppression is being 35 dB.

2.2. Operational Experience

The final amplifier, as shown in **fig. 8**, has been used by the author in FM relay and in SSB working for over a year now with no problems whatsoever. The advantage of the unit lies in its wideband characteristics and in its robustness.

The prototype of the double PA has been in constant use for over a year in a 23 cm FM-relay operation. It sometimes occurs that it is overdriven for periods of more than 10 hours at powers of 45 W but, as yet, with no problems. If the construction is carried out exactly in accordance with this article, there is nothing to prevent an entirely successful operation with this unit. Again, do not use any cut-outs in the housing cover.

A must for all active and technically minded Radio Amateurs!

THE UHF-COMPENDIUM

The English edition of the well-known "UHF-Unterlage" from Karl Weiner, DJ 9 HO.

Part 1 and 2

Art.No. 8054

DM 52.00

Part 3 and 4

Art.No. 8055

DM 58.00

Additional post and package charges (surface mail) for inland DM 5.00, for abroad DM 6.50.



Telecommunications, VHF-Communications - UKW-Technik Terry D. Bittan
Jahnstraße 14, D-8523 Baiersdorf, Telefon (09133) 470, Telex 629887



Matjaž Vidmar, YT 3 MV

Digital Signal Processing Techniques for Radio Amateurs

Part 4 b: Application Software

4.3. APT/WEFAX PICTURE RECEIVING AND PROCESSING SOFTWARE

As described in the introduction (theory) article, the DSP computer was first intended for the reception and processing of weather-satellite pictures. The DSP computer video board was designed to generate the highest-resolution picture that is still compatible with standard TV monitors: 256 lines of 512 pixels with 256 grey levels per pixel.

After a few experimental programs to test different demodulation and synchronization DSP routines, two final application programs were developed. The APT program was designed for the reception of pictures from polar orbiting satellites. It allows the recording of a single APT picture at full resolution and a comprehensive picture processing afterwards: zooming and grey-scale enhancements. The other program, WEFAX, was designed to receive sequences of pictures from geostationary satellites like

METEOSAT. To save memory space, WEFAX does not allow zooming after pictures have been recorded. It can, however, record sequences of up to 14 pictures (with 1 Mbyte of memory) that can be displayed in a moving sequence.

Both programs have in common a high performance DSP demodulator (with a look-up table), an automatic and very accurate gain/grey scale adjustment routine and reliable and accurate synchronization routines. Since pictures require by far the largest amount of memory, they are stored in separate files. Both programs include routines to create suitable picture files according to the available memory.

The APT program includes 15 user defined picture formats as shown in the main menu in **fig. 3.1**. It, however, works with a single-picture file containing a single picture at a time. If a file with the specified file name does not exist, the program will allow the user to create such a file. The length of the latter will of course be limited by the available memory. The length of the file is displayed as the number of bytes in hexadecimal format. The program uses one byte per pixel of the picture stored. The organization of pixels into lines, however, depends on the selected picture format.



The structure of a (user-defined) picture format is shown in **fig. 3.2**. A picture format essentially consists of two parts: the recording parameters and the display parameters. The recording and signal parameters should be set up before attempting to record a picture. Internally, the program is sampling the APT signal at a rate of 4800 pixels per second. For a 240 lines per minute APT signal this means that one line is 1200 pixels long and this information has to be provided to the computer! The computer should also know what is the sync burst frequency and duration to be able to synchronize the picture.

The recording parameters define the resolution and the length of the picture stored in the file given a certain amount of memory. For instance, if 512 kbytes (80000H bytes) of memory are available and 1024 pixels per line are stored, the picture file will contain a picture of 512 lines. If the picture is to be recorded at reduced resolution, then the pixel and line sampling rates are to be set accordingly. The format allows for an offset of the start pixel to avoid recording the sync pulse at the edge of the picture. If the picture is recorded at reduced resolution, the program performs an automatic averaging to improve the signal-to-noise ratio.

The display parameters define the processing of the stored picture for display. They can be edited like the recording parameters or modified interactively during picture display. The display parameters allow independent zooming in the two directions, moving the display window around the picture and grey scale enhancement.

The program performs a check of all format parameters immediately after any parameter is modified. If some parameters are found out of bounds they will be modified to the nearest acceptable value. In particular, the internal line buffers are limited to 2700 pixels and the program can not accept picture formats slower than 120 lines per minute. Slower formats, used in the past (ITOS satellites, old METEOR-2 IR) are seldom used today: larger line buffers would only result in unnecessary waste of memory.

To record and/or display a picture, a picture file with the specified name must exist and a picture format has to be selected. Selecting a picture format starts two independent tasks: a picture recording task and a picture display task. To start recording a picture a manual start command has to be issued. This will first start a synchronization routine as indicated in the annotation line below the picture.

*** ITOS - APT (EFW) 3.4 kHz subcarrier FX - 10/07/1998 ***

```

Picture Format menu
-----
Picture format: 1
Picture file name: METEOR.PIC
Picture file length: 80000
Write offset: 0
Start pixel offset: 77000
@ or carriage return = exit
Insert format number or option:
    
```

Fig. 3.1.: APT program main menu

```

***** Picture Format number 1 @ *****
| Format name: METEOR-1 240
*** Signal parameters @ 4800 pixels per second ***
Line length: 1200 pixels
Sync frequency: 1200 Hz
Sync burst length: 23 pixels
*** Recording parameters ***
Pixel sampling rate: 1.00 pixels
Line sampling rate: 1.00 lines
Recorded pixels: 1024 per line
Start pixel number: 11 pixels
*** Display parameters @ 512 pixels per line ***
Pixel sampling rate: 0.500 pixels
Line sampling rate: 1.000 lines
Start pixel number: 200 pixels
Expansion sign: 1
Expansion offset: 200 - 255
14 Copy picture format: add format number
@ or carriage return = exit to main menu
Insert parameter number or option:
    
```

Fig. 3.2.: Editing APT picture format

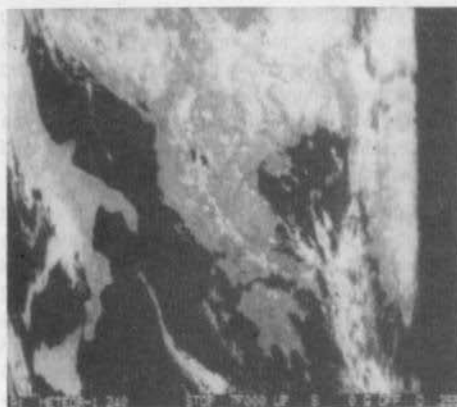


Fig. 3.3.: APT picture display (no grey levels)

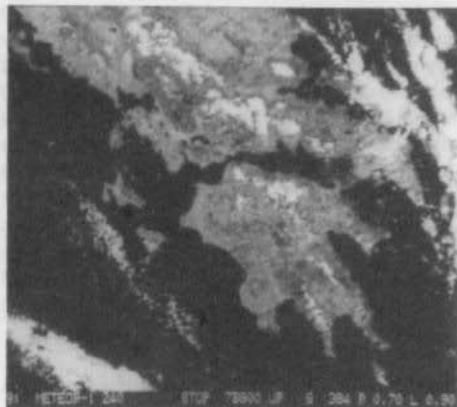


Fig. 3.4.: APT picture display, enlarged

The synchronization is achieved by computing the cross-correlation between the defined sync pattern and the average of 8 successive lines. The synchronization routine may take a few seconds to find the best match. The recording will start afterwards at the write offset as displayed in the annotation line. Before issuing the start command, the write offset usually has to be reset first! The recording will stop automatically when the write offset reaches the end of the picture file: when there is no more memory space available.

The picture display window includes 248 lines of 512 pixels each since the bottom 8 display lines are used for the annotation line (see figs. 3.3. and 3.4.). The display has two modes of operation. In the AUTO mode, the display window tracks the recording operation and the last recorded information is displayed. In the MAN mode, the display window can be moved in any direction along the picture. All other commands are available in both modes. As usual, in the case of a wrong command, the "On-line HELP" message is displayed (fig. 3.5.). The display is updated between 1 and 5 times per second, depending on the computer loading. The effects of zooming and grey scale enhancement can therefore be noted immediately.

The grey scale enhancement function requires two parameters: gain and offset. Offset specifies

a value between 0 and 255 where the specified gain increase will occur. The program will then compute a transformation function such that no saturation occurs either below or above the point of the gain increase; of course the gain has to be decreased in these regions. The function itself is of the form $Y = X/\text{SQRT}(X^2 + 1)$, which is shifted and stretched to match both end points and the required gain increase at the required offset at the same time.

XXXXX Recording & Display Immediate Commands XXXXX

```
TEI  COMMAND
CR      Exit to main menu | STOP only
+       Sync & Start recording
-       Stop recording
*       Picture UP / DOWN
/       Sampling rates / Expansion parameters
@       Display address AUTO / MAN
@+      Display address + 1 line  MAN only
@-      Display address - 1 line  MAN only
@J      Start pixel number + 1 pixel
@L      Start pixel number - 1 pixel
@MN     Pixel sampling rate + 0.001 / Expansion gain + 0.001
@MN     Pixel sampling rate - 0.001 / Expansion gain - 0.001
@O+     Line sampling rate + 0.001 / Expansion offset + 1
@O-     Line sampling rate - 0.001 / Expansion offset - 1
@R      Reset recording address offset
( )     MAN Phasings
To exit press any key!
```

Fig. 3.5.: APT program "On-line HELP"



Fig. 4.3.: WEFAX picture display

Of course, to edit a picture format the latter has to be deactivated and disabled first! Similarly, the format has to be enabled afterwards to allow the automatic recording of pictures. Selecting a particular picture format from the main menu will show the recorded picture sequence (fig. 4.3.) if a picture file with the given name exists. It is not necessary for the format to be enabled to display the picture sequence: for example, if it is not desired to write any new pictures to the file.

```
xxxxxx DISPLAY COMMANDS xxxxxx

KEY  COMMAND
CR   Exit to main menu
+    Next picture
-    Previous picture
0    Stop scanning
1 to 9 Set scanning speed / 1 = highest scanning speed
U    Increase gain - contrast
D    Decrease gain - contrast
W    Increase offset (towards white)
B    Decrease offset (towards black)

xxx Press any key to exit!
```

Fig. 4.4.: WEFAX program "On-line HELP"

On the other hand, the display operation does not influence the picture recording task either. When a new picture is overwriting an old one, the two pictures will be separated by a dotted line. The annotation line at the bottom will only be updated with the time and date of the new picture after the complete new picture was transferred to the file.

In the picture display mode, the user can either manually scan the pictures contained in the picture file or set the scanning speed for automatic scanning. A grey-scale enhancement routine identical to that in the APT program is provided as well. A wrong command calls the "On-line HELP" as in fig. 4.4.

WEFAX.SRC is about 18 kbytes long. When compiled into an executable file, it requires about 97 kbytes of memory. "Full" pictures take about 128 kbytes each while "economy" pictures only take about 64 kbytes of memory each. With 1 Mbyte of memory this means either 7 "full" pictures or 14 "economy" pictures or a combination of both. Unfortunately, with a single memory board (256 k) there is only room for 1 "full" or 2 "economy" pictures, since the program must be present too.

Future additions to WEFAX may include a similar picture handling as in the APT program, where zooming can be performed also after the pictures have been recorded. This however requires much more memory. A routine to automatically synchronize the computer real-time clock could be added easily: picture start times are usually accurate!

Finally, there are many other picture transmission formats a DSP-oriented computer could demodulate and display. LF and HF FAX transmissions and radio-amateur SSTV are particularly interesting. The FAX standard is used many times to transmit just black-and-white maps: a considerable saving of the required memory space could be made by storing just 1 bit per pixel. SSTV is just a derivative of the HF FAX standard: due to the low resolution of SSTV pictures, available memory space would not be a problem either. The computer could easily transmit in any of the mentioned standards as well, so there are many possibilities for further developments.



```

xxx Y3M - PSK/M 1200 bps AX,25 modem - 22/06/1999 xxx

1 Receive / Transmit

0000 Receive file : PSK1200 .TXT
0001 Transmit file :
0002 File length : FILE DOES NOT EXIST

4 Call : 801045
0003 My call : Y3M
0004 Dist(s) :

7 TX amplitude : 330
Header length : 1664 flags
TX delay :
ACK delay : 8000
Packet size : 4 frames
Frame length : 8000 bytes
Retry :
Link(s) :
Bit rate : 1111
Carrier : 1200 Hz
Screen format : 64 columns

17 Set default parameters

0 on carriage return = exit

Enter option number : #

```

Fig. 8.1.: PSK 1200 packet radio program main menu

received frames. Therefore there is no critical adjustment of the transceiver's squelch to be performed like with commercial TNC DCDs and no related delay either! On the other hand, it is always necessary to adjust the amplitude of the output signal to correctly modulate the trans-

```

xxx Y3M - Manchester AX,25 modem - 25/06/1999 xxx

1 Receive / Transmit

0000 Receive file : MAX25 .TXT
0001 Transmit file :
0002 File length : 344 bytes

4 Call : Y3M-1
0003 My call : Y3M
0004 Dist(s) :

7 TX amplitude : 220
Header length : 330 flags
TX delay :
ACK delay : 1666
Packet size : 4 frames
Frame length : 8000 bytes
Retry :
Link(s) :
Bit rate : 2400 bps
Carrier : 2400 bps
Screen format : 64 columns

18 Set default parameters

0 on carriage return = exit

Enter option number : #

```

Fig. 9.1.: MAX 25 packet radio program main menu

```

xxx RX PSK - TX Manchester AX,25 PSK 1200 bps xxx

xxx CON CHD xxx

xxx CON FAILURE xxx

xxx Error !!! Valid commands are : xxx

Dev CHD MODE TX MODE
-----
+-----+-----+-----+
| TX ON / OFF | Chn |
| CALL ON / OFF | Chn |
| CON CHD | Chn |
| DISC CHD | Chn |
| Transmit file | Chn |
| REC ON | Chn |
| REC OFF | Chn |
| Print REC length | Chn |
| Tuning ON / OFF | Chn |
| Exit | New line & Transmit Frame |
| Switch to TX MODE | Switch to CHD MODE |
+-----+-----+-----+

xxx REC ON xxx

xxx CON CHD xxx

xxx CON FAILURE xxx

#

```

Fig. 8.2.: PSK 1200 program error message – "On-line HELP"

mitter: the parameter TX amplitude has to be set according to the transmitter used.

PSK 1200 and MAX 25 have some additional parameters to be set. PSK 1200 allows the PSK demodulator carrier frequency to be adjusted between approximately 1200 and 1800 Hz. MAX 25 allows both receive and transmit bit rates to be set independently, of course within certain limits (to be discussed later).

An example of using the AX 25 program is shown in **fig. 7.2**. In operation the packet-radio programs can be switched between two modes. In the command mode characters entered from the keyboard are decoded as commands. Any errors call an "On-line HELP" message as in **fig. 8.2**. In the text mode all characters are considered as text to be transmitted. The switch-over between the two modes is performed by the line-feed key (CTRL-J). The latter was chosen since it is seldom used; depressing carriage-return already generates a CR/LF on the screen.

During information transfer in the connected state, the blinking cursor symbol is replaced by a blinking number. This number indicates the number of frames in the transmit queue that have not been acknowledged yet. After all frames have been acknowledged, the cursor is again



replaced by its standard symbol. This feature allows an immediate check of the status of the contact and/or channel loading; its function corresponds to the ACK LED on commercial TNCs.

PSK 1200 requires accurate tuning when used with SSB receivers (± 200 Hz), therefore it includes a tuning indicator identical to the BPSK 400 program. No accurate tuning is required with the other two programs, AX 25 and MAX 25, since they are usually used with FM transceivers.

MAX 25 is an experimental program and its demodulator works with just 4 signal samples per bit. The DSP routine is using interpolation between samples to achieve synchronization. The MAX 25 demodulator is therefore very sensitive to the input signal filtering. The TP 3040 input filter on the analog I/O board is not ideal for this application: it has a large differential group delay and severely distorts the signal. With the TP 3040 filter MAX 25 achieves acceptable results at 2400 bps. Replacing the filter, MAX 25 can be used for any speed up to 3200 bps.

All three packet-radio program sources are each around 21 kbytes long. When compiled they require from 73 to 75 kbytes of memory each. Future developments include experiments with new modems. AX 25 could be readily modified for 300 bps HF operation and equipped with the same tuning indicator as the RTTY program, since it uses the same DSP demodulator routine. However, the BELL-103 standard, presently used on HF, is not the best suited for the HF propagation, medium and further experimentation will be necessary including much more sophisticated DSP techniques, before a reliable standard can be selected. On the other hand, 2400 bps is certainly not the highest speed that can be obtained in a voice bandwidth channel. A QPSK modem would probably work up to 4800 bps and other techniques could be used to go beyond this figure. Finally, a packet-radio program without a DSP modem, using the high-speed serial port should be developed for high-speed microwave packet communications.

4.6. CONCLUSION

All the software, described in this article, was extensively tested and its operation is considered reliable. All the software was developed along the same guidelines: a wrong command displays a HELP message immediately and a carriage-return causes an exit. In a few words, on a working hardware, users should never need to press the RESET button!

All the software presented has similar hardware requirements: CPU board, video board, analog I/O and floppy drive. The floppy drive is only used to load programs, the latter could also be loaded from another similar computer through the RS-232 port thus eliminating the need for the floppy drive and related controller. All software can work with a single 256 kbyte memory board, although in this case the performance of weather-satellite picture processing programs will be rather limited. The more memory the better but unfortunately, due to the recent static RAM shortage and related speculation, the prices are very high. All software is ready to work with the full addressing range of the microprocessor of 16 Mbytes (less the space taken by the operating system). No program is using the high-speed serial port yet: the related components simply need not be installed yet.

From the publication of the previous article, an improved version of the operating system, V7.2 was developed. It is completely compatible with all previous software and includes only additions. It still fits on a 16 kbyte EPROM so it can be supplied on 27128, 27256 or 27C256 EPROMs. The operating system manual was not only updated but also enlarged: in particular it includes a much more detailed description of the high-level language compiler.

Application software can be supplied on both 3.5" floppies (800 k per floppy) or 5.25" floppies (400 k per floppy). The floppy controller and operating system software can use both types of floppy drives with no modifications, but 3.5" floppy drives are recommended for obvious reasons.



All radio-amateur DSP software (all the software described in this article) is intended to be "PUBLIC DOMAIN SOFTWARE". It can therefore be copied freely and is available both from the author and from the publishers for just the expense for the media (floppy), handling and postage. Modifications and additions to these programs are encouraged and further advice can be obtained from the author by either writing or calling to the given address/phone number:

**Address: Matjaž Vidmar, YT 3 MV
S. Masere 21
YU-65000 Nova Gorica
Yugoslavia
Phone (home): (+ 38) 6526717**

This article describes the presently available software. It already includes the description of probable additions and new developments in each software group. Other software is in development too. When ready, it will be described in future articles and made available.

4.7. REFERENCES

- (1) J. R. Miller, G 3 RUH:
"OSCAR-10 POSITION CALCULATION PROGRAM",
Oscar News 45, December 1983, p. 15 - 18,
AMSAT-UK
- (2) Silicon Solutions: "GRAFTRAK",
set of tracking/display programs for IBM
compatibles.
- (3) Terry L. Fox, WB 4 JFI:
"AX.25 Amateur Packet-Radio
Link-Layer Protocol, Version 2.0",
October 1984, American Radio Relay
League, Inc., Newington, CT USA 06111
- (4) Klaus Eichel and Hans-L. Rath:
GrafTrak and Mirage Interface (MTI) —
Something Really Good for the Radio
Amateur
VHF COMMUNICATIONS Vol. 20,
Ed. 2/1988, P. 66 - 84 and
Ed. 3/1988, P. 171 - 178



We accept **VISA Credit Card, Eurocard**
(Access/Master Card) and only require
the order against your signature, card
number and its expiry date.

VHF COMMUNICATIONS / UKW-BERICHTE



UKWberichte

T. Bittan OHG · Jahnstr. 14 · P.O.Box 80 · D-8523 Baiersdorf
Tel. West Germany 9133 47-0. For Representatives see cover page 2

Hans Michl, Heilbronn

2.83 GHz DR-Oscillator

In reference (1) YT 3 MV described an antenna pre-amplifier and converter for the TV-satellite range at about 4 GHz. He employed a bipolar local oscillator which worked above the received frequency and in stripline technology. Just as a matter of interest, an oscillator will now be described which has its frequency determined by a dielectric resonator (DR) but which operates under the received frequency. The principle of operation of the dielectric resonator has already been covered in (2) and therefore only the practical details of this circuit will be dealt with here.

1. CIRCUIT DETAILS

In order that the received frequency range of 3.6 to 4.2 GHz can be translated to an IF of about 0.8 to 1.4 GHz, a converter local oscillator frequency of 2.8 GHz is required. This could be realized by using a Siemens DR with a nominal frequency of 2.83 GHz.

The circuit is given in **fig. 1** in the form of a general layout sketch together with the connections for

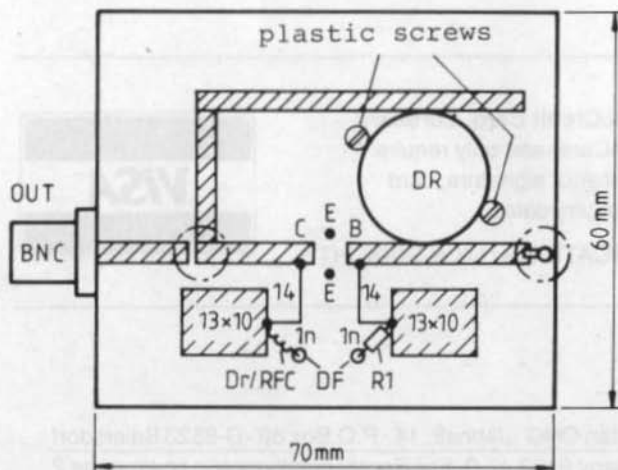


Fig. 1:
RF circuit diagram
of the 2.8 GHz
oscillator

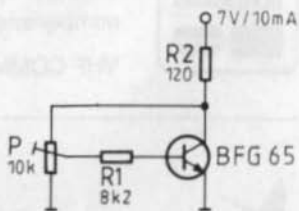


Fig. 2:
DC connections to the
oscillator transistor

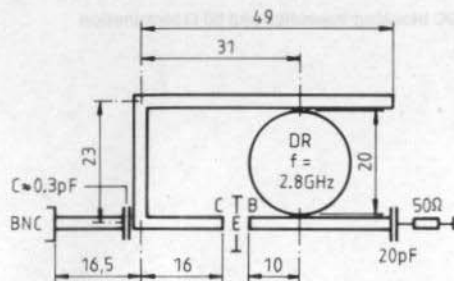


Fig. 3: Dimensions of the striplines and the position of the DR

the microwave transistor **BFG 65**. The latter works with a supply voltage U_B of 7 V and collector current I_C of 10 mA. The oscillator delivers an output power of 6 dBm at a frequency of $f = 2.838$ GHz. The power output is sufficient to drive a ring mixer and the author used the Mini-Circuits type PAM-42.

The DC connectors are detailed in the diagram of **fig. 2**. The wiper of the preset pot'meter P1 is connected to the base feed-through insulator. The collector feed-through is connected to R2 and the higher end of P1. The collector RFC comprises 5 turns of 0.3 mm copper lacquered wire (CuL).

The DR has the effect in this circuit of a selective transfer from the stripline at the transistor output to the transistor's input stripline. The resonator's position determines the feedback phase and its height above the stripline controls the degree of feedback. In order that the conditions for oscillation are fulfilled, a phase reversal of 180° must be achieved in which the transfer angle of the transistor's (S_{21}) must be controlled. Owing to the velocity factor of the 50Ω stripline, its physical dimensions would be inconveniently short to produce 180° phase change, therefore the dimensions were increased to produce a 540° ($180^\circ + 360^\circ$) reversal.

This circuit will not oscillate without the DR. Even with the DR mounted at a height of 3.5 mm over the stripline, the feedback coupling is so loose that the circuit fails to oscillate. The conditions for oscillation are only satisfied when the module cover is in position. This intensifies the field

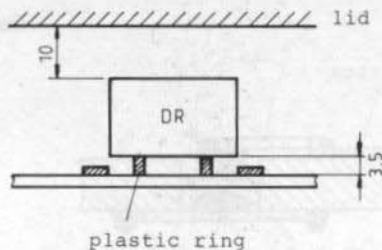


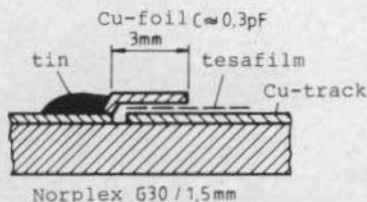
Fig. 4: The DR's construction. Two plastic securing screws are used.

around the tuned conductors. Owing to the loose coupling, the circuit Q is extremely high which accounts for the good suppression (26 dB) of the second harmonic output and also its low phase noise about the fundamental frequency.

In-depth testing for drift and phase noise could not, however, be carried out owing to the lack of suitable test equipment. For the author's application, drift was not too critical as the satellite TV system bandwidth is very large (27 MHz).

2. CONSTRUCTION

The circuit was constructed on epoxy-glass material G30 (NORPLEX-Europa in Wipper-



output coupling capacitor

Fig. 5: Output coupling capacitor

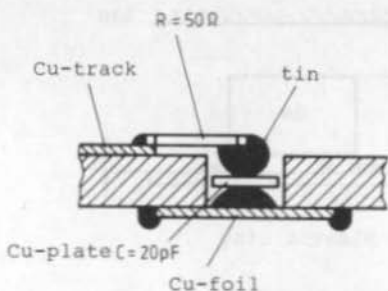


Fig. 6: DC blocking capacitor and 50 Ω termination

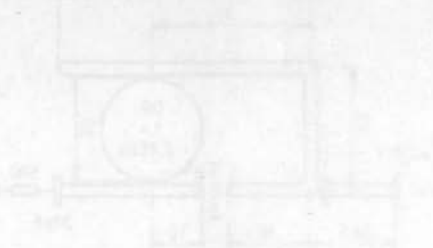


Fig. 7:
Oscillator module from above

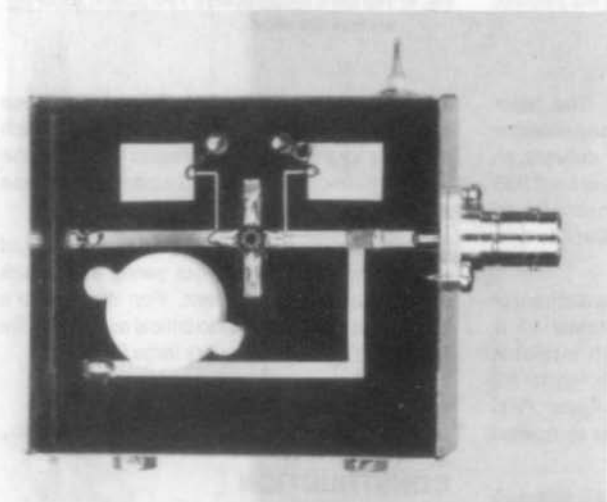
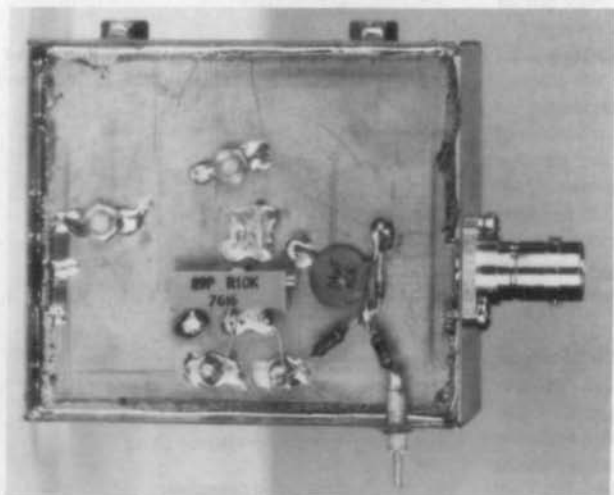


Fig. 8:
Oscillator module from below





fürth). The relevant data for the striplines is:—

$$\epsilon_r = 5.0$$

$$\text{Velocity factor} = 0.55$$

$$h = 1.4 \text{ mm}$$

This is for a Z_0 of 50 Ω

$$w = 2.6 \text{ mm}$$

Fig. 3 shows all the necessary dimensions and fig. 4 shows the positioning of the resonator. The indicated cover in fig. 4 belongs to a tin-plate box having internal dimensions of 60 x 70 x 30 mm.

Both the choke (RFC) connections from base and collector leads to the etched de-coupling capacitor (13 x 10 mm) are $\lambda/4$ PCB tracks with a characteristic impedance of around 120 Ω , ($w = 0.5 \text{ mm}$).

The construction of a microwave coupling capacitor is shown in fig. 5. The diagram of fig. 6 shows the detail of the base stripline

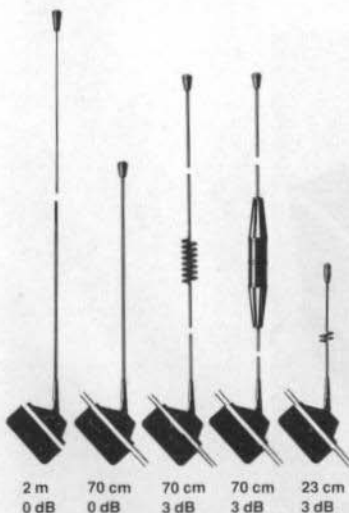
termination using a 50 Ω SMD resistor and a plate capacitor.

The photograph of figs. 7 and 8 show the construction by above and below perspectives.

3. REFERENCES

- (1) Vidmar, M., YT 3 MV:
Receiving Converter for 4-GHz-Band Satellite
VHF COMMUNICATIONS Vol. 20,
ed. 2/1988, p. 103 - 110
- (2) Jirmann, J., DB 1 NV and Krug, F., DJ 3 RV:
The Dielectric Resonator
VHF COMMUNICATIONS Vol. 15,
ed. 4/1983, P. 194 - 201

GF 151 GF 401 GF 404 GF 411 GF 23-3



GlassFix[®] Antennas

A small selection of our wide range of mobile antennas

- * Require no holes in your car
- * Transmit through glass
- * No ground plane required
- * Performance equal to roof mounted antennas
- * Can be removed leaving no trace of the installation
- * Re-installation kit available

Model	GF 151	GF 401	GF 404	GF 411	GF 23-3
Type	$\lambda/2$	$\lambda/2$	collinear	collinear	collinear
Frequency	138 - 175 MHz	430 - 470 MHz	430 - 470 MHz	430 - 470 MHz	1240 - 1300 MHz
Gain	0 dB	0 dB	3 dB	3 dB	3 dB
max. power	25 W	25 W	25 W	25 W	25 W
Cable	4 m RG 58	4 m RG 58	4 m RG 58	4 m RG 58	4 m RG 58
Length	85 cm	25 cm	66 cm	66 cm	17.5 cm
Art.No.	0163	0164	0165	0168	0166
Price	DM 98.00	DM 83.00	DM 95.00	DM 99.00	DM 110.00



Roman Wesolowski, DJ 6 EP

9 cm-Band Tube PA Stage

The following article about a two-stage power amplifier using a tube, should serve two purposes; the spur to more experimentation and also to increased activity on the 9 cm band. The previously published 9 cm PA was based on the triode YD 1060 and which has now been developed to give a maximum output of 10 W. The search for a more powerful tube was finally concluded with the extremely robust 2C39BA. This triode is specified up to a fre-

quency of 3 GHz but at this limit there is somewhat of a compromise. The RF output power of 40 W, however, was sufficient argument to put it into operation despite some operational difficulties. The photograph of fig. 1 shows the prototype.

The 16 dB power gain, at an output power of 17 dBm, fell to 11 dB at full output power thus making the use of a valve driver stage mandatory.

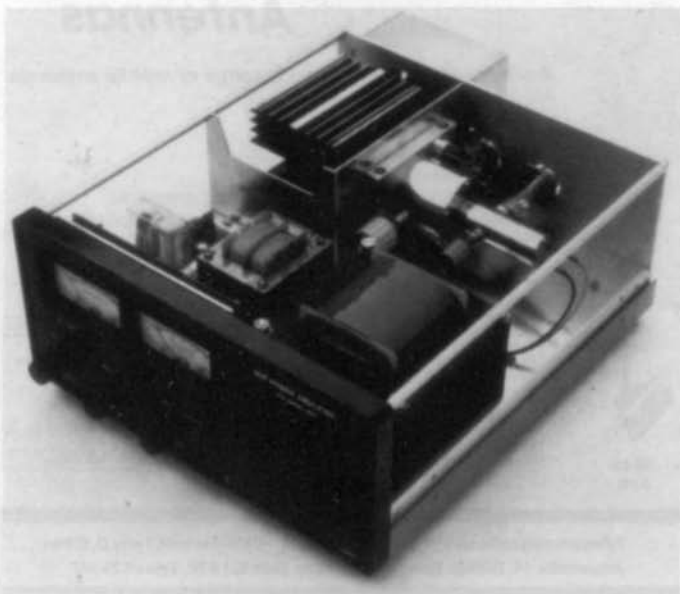


Fig. 1:
The completed 9 cm
PA stage using the
2C39BA

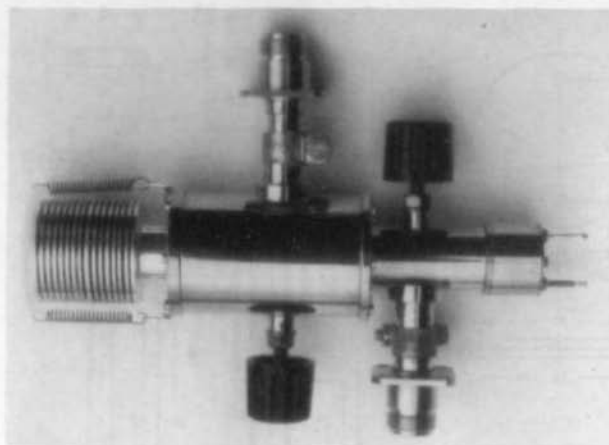


Fig. 2:
The (driver) stage using the YD 1060

It was no particular trouble to construct this from new as good results had already been obtained from the YD 1060 in a coaxial construction at

6 cm and it was only necessary to redimension it for 3.4 GHz. The photograph of fig. 2 shows the completed pen-ultimate amplifier. This driver,

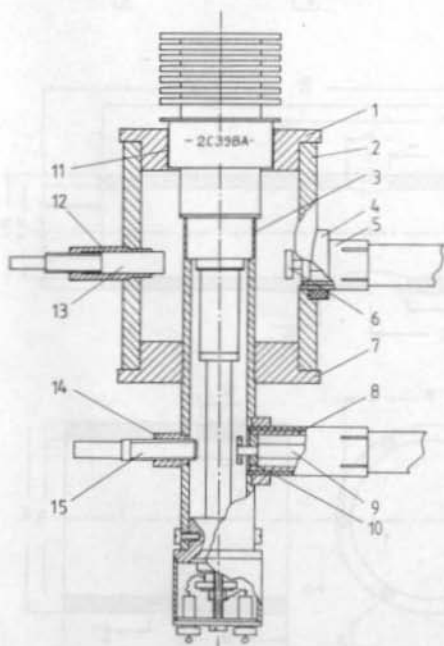


Fig. 3: Overall cross-section of 9 cm PA with 2C39BA

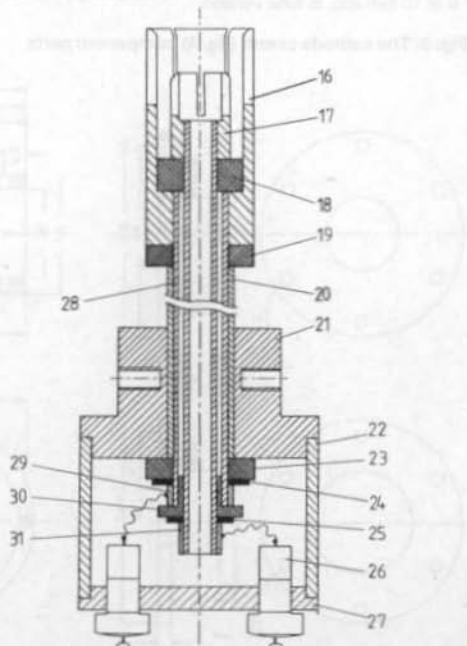
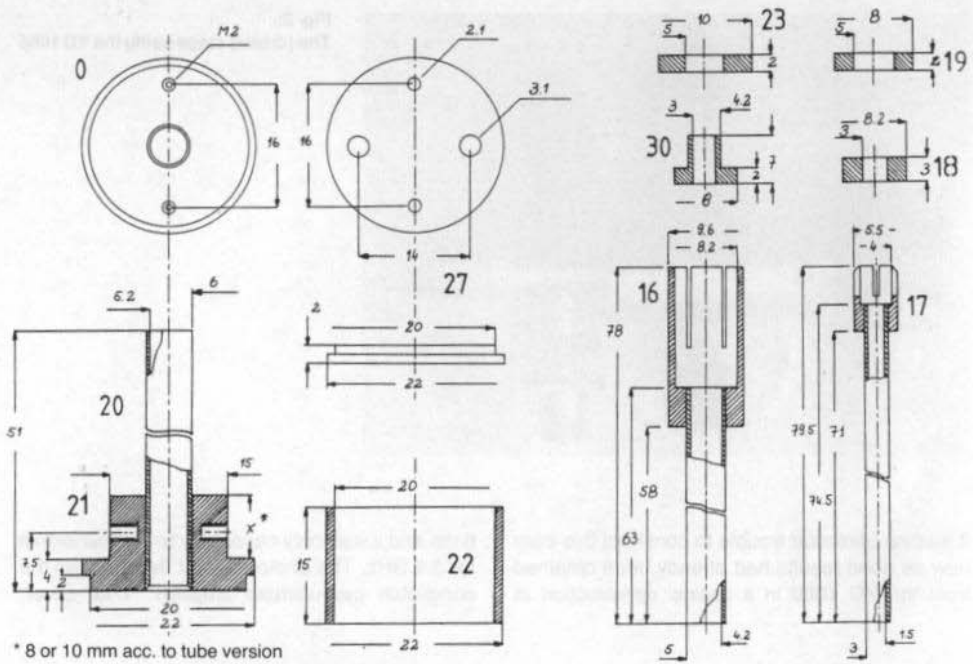


Fig. 4: Cathode circuit of the 9 cm PA with 2C39BA



* 8 or 10 mm acc. to tube version

Fig. 5: The cathode circuit (fig. 4) component parts

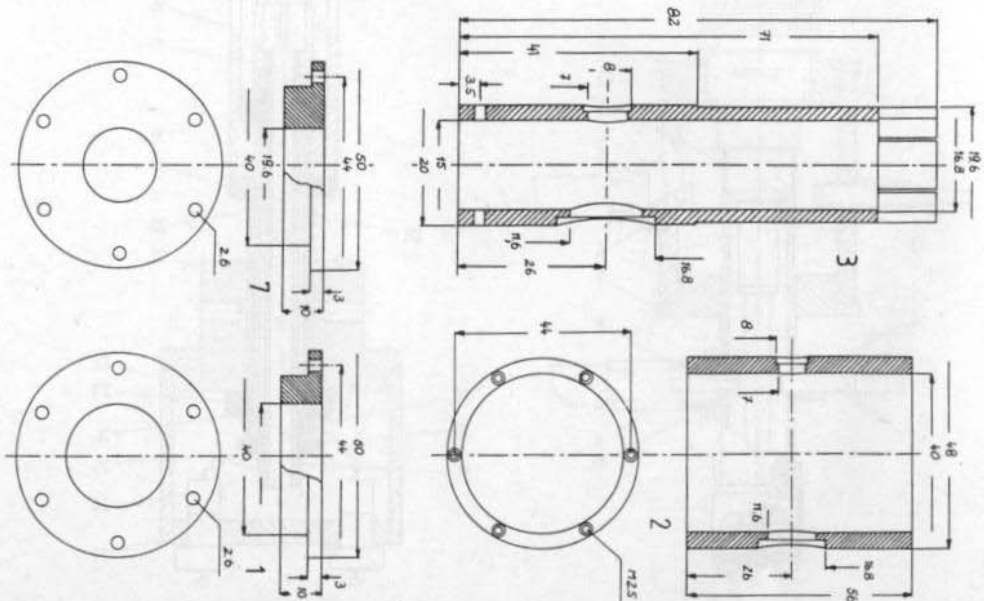


Fig. 6: Grid cylinder, anode cylinder, anode cylinder top cap, anode cylinder bottom cap (fig. 3)

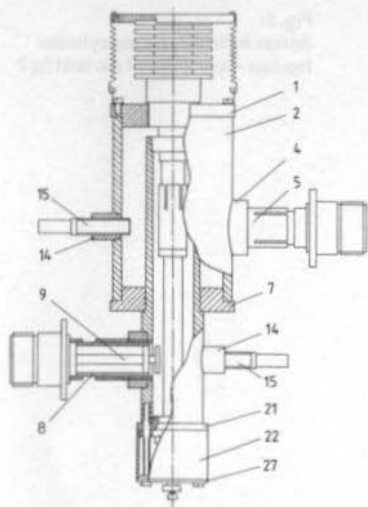


Fig. 7: Overall cross-section of the 9 cm PA (driver) with the YD 1060

together with the PA stage, gave an overall gain of 23 dB. At this point, it may be mentioned that parallel experiments with the triode TH 316/TH 326 gave grounds for optimism. For 30 W output, the power gain was 7 dB which made it a good alternative to the 2C39 final stage. As no good tubes were available, all experiments were postponed.

1. SPECIAL DETAILS

As both amplifiers are practically identical with the 6 cm stage detailed comprehensively in (1), only a few particular points will be mentioned. All the

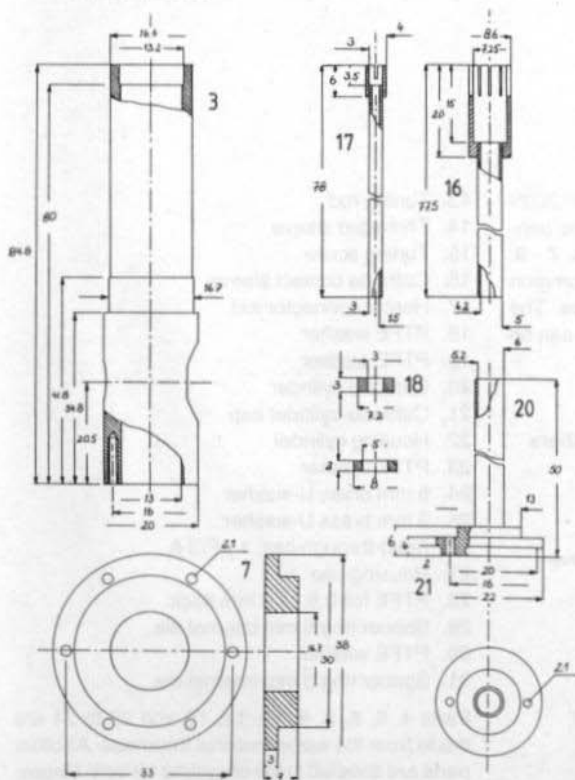


Fig. 8: Grid cylinder, anode cylinder bottom cap, component parts of cathode circuit — all details of fig. 7

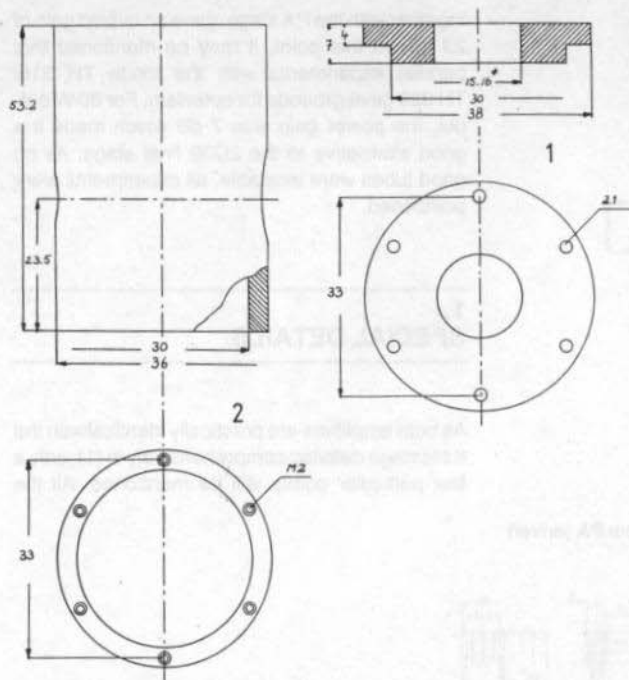


Fig. 9:
Anode cylinder, anode cylinder
top cap – component parts of fig 7

required details for the power amplifier 2C39 are given in **figs. 3 - 6** and those for the penultimate stage YD 1060 are given in **figs. 7 - 9**. The diagrams of **fig. 10** represent the common components for both driver and PA stages. The parts not identified in the driver diagrams can be obtained from those of the PA stage.

1.1. Important-Parts List for both Amplifiers

- | | |
|---|-------------------------------------|
| 1. Anode-cylinder top cap | 13. Tuning rod |
| 2. Anode cylinder | 14. Threaded sleeve |
| 3. Grid cylinder | 15. Tuning screw |
| 4. Mounting ring for output coupling sleeve | 16. Cathode contact sleeve |
| 5. Output coupling sleeve | 17. Heater connector rod |
| 6. Coupling probe disc | 18. PTFE washer |
| 7. Anode-cylinder bottom cap | 19. PTFE washer |
| 8. Input coupling sleeve | 20. Cathode cylinder |
| 9. Input coupling rod | 21. Cathode-cylinder cap |
| 10. PTFE washer | 22. Housing cylinder |
| 11. Anode dielectric isolator (PTFE foil) | 23. PTFE washer |
| 12. Threaded sleeve | 24. 5 mm brass U-washer |
| | 25. 3 mm brass U-washer |
| | 26. Feed-through cap. 1 μ F/3 A |
| | 27. Housing cap |
| | 28. PTFE foil 0.8 - 1.0 mm thick |
| | 29. Spacer ring 5 mm internal dia. |
| | 30. PTFE washer |
| | 31. Spacer ring 3 mm internal dia. |

Parts 4, 5, 6, 8, 9, 10, 14, 15 and 22 to 31 are made from the same material thickness. All other parts are detailed in the diagrams for both stages.

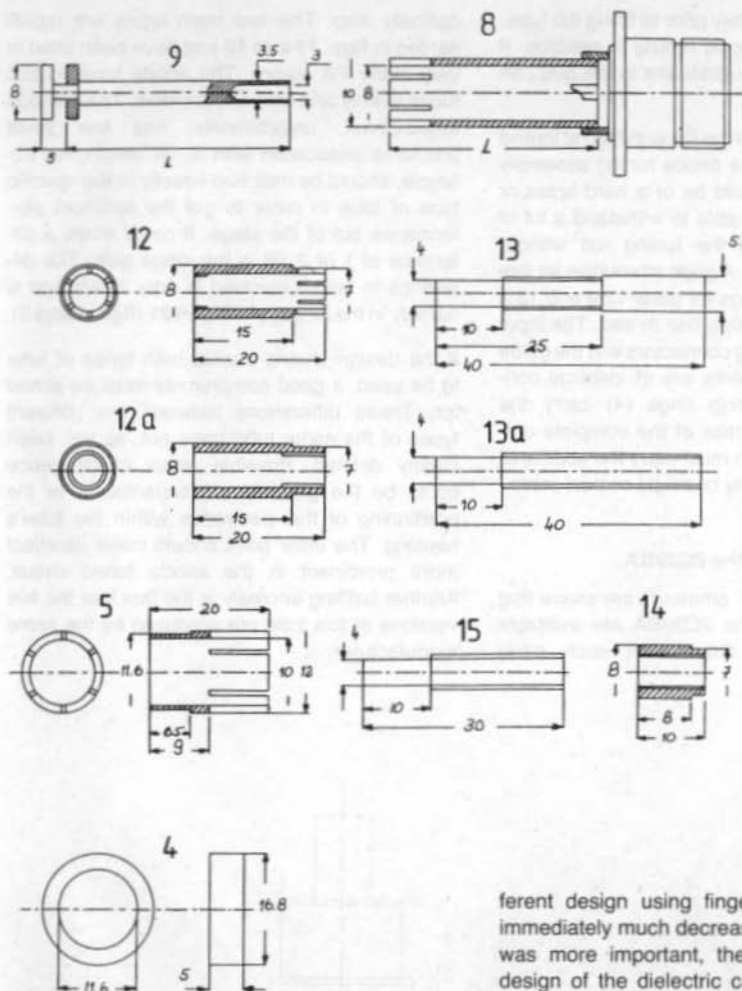


Fig. 10:
Parts common
to both
aplifier
versions

1.2. Anode Dielectric

The prototypes of this project were introduced to small gatherings of "experts" and were then the subject of discussion. A few of the ideas emanating from this discussion were tried out in practice by the author. One of these was the rather tricky business of forming an anode dielectric capacitor which had to be carried out in a straight-forward conventional manner. The anode top cap of the completed 2C39 PA was replaced, for trial purposes, by a radically dif-

ferent design using finger-contact stock. This immediately much decreased the gain, but, what was more important, the efficiency also! The design of the dielectric capacitor is one of the main reasons for this deterioration and it can be said that the success of the entire design hangs upon this single factor. The entire inner diameter of the anode cylinder top cap should be covered by the PTFE foil. The foil should not be thicker than 0.15 mm. The dimensions of the valve's anode rings must be rigidly controlled.

1.3. Grid ring, Tuning rod, Input-Output Coupling

The seating of the grid ring at the end of the cathode sleeve should be coated with con-

ducting silver immediately prior to fitting the tube. This seems to bring good results in practice. If this is done, the longitudinal slot in the grid can be dispensed with.

The anode tuning rod of the PA is slotted at its end and force-fitted into the anode tuning assembly sleeve. The latter should be of a hard brass or bronze stock which is able to withstand a lot of tuning movements of the tuning rod without showing signs of wear. A good alternative for this is shown in the drawings for parts 12 a and 13 a which are provided with a fine thread. The input and the output-coupling connectors and the guide sleeves of both amplifiers are of identical construction. The mounting rings (4) carry the highest mechanical stress of the complete output assembly (5) which must carry the additional burden of a coaxial relay or a rigid coaxial cable.

1.4. Two Versions of the 2C39BA

All well-seasoned VHF amateurs are aware that several versions of the 2C39BA are available commercially which differ from each other

optically also. The two main types are represented in **figs. 11 and 12** and have been used in very many PA stages. The anode tuned-circuit tunes evenly and with no problems. The cathode tuned-circuit, unfortunately, has few small problems associated with it. Its length, for example, should be matched exactly to the specific type of tube in order to get the optimum performance out of the stage. It could make a difference of 1 or 2 dB in the stage gain. The difference in length involved is only 2 mm and is namely in the length of the part 21 (**figs. 4 and 5**).

If the design should enable both types of tube to be used, a good compromise must be aimed for. These differences between the different types of the same tube have not, as yet, been clearly defined. Possible areas of difference could be the grid-cathode capacitance or the positioning of the electrodes within the tube's housing. The latter point should make its effect more prominent in the anode tuned circuit. Another baffling anomaly is the fact that the two versions of this tube are produced by the same manufacturer.

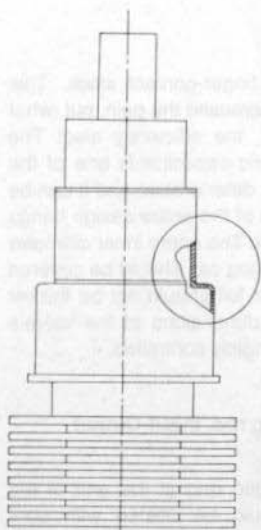


Fig. 11:
Tubes version 1:
dimension X for part
21 (fig 5): 8 mm

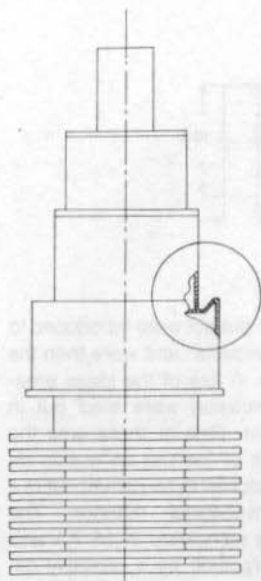


Fig. 12:
Tubes version 2:
dimension X for part
21 (fig 5): 10 mm



1.5. Cooling

There is a problem associated with the cooling of the 2C39. Even during the experimental stage it became clear that the amplifier was not thermally stable. At a DC input power of 200 W, the variation in inter-electrode capacitance was naturally more noticeable than operation at 13 cm or 23 cm. The possibility of providing water-cooling (3) was considered, but the increased complexity and work involved did not seem to justify the increase in power output which would have resulted. The following measures go a large way to solving the cooling problems which result in a usable and relatively powerful final stage.

A stable, aluminium clamp was fitted to the middle of the PA's chassis. The radiator fins of the triode were replaced by a copper block which was secured in close contact with a large aluminium heat-sink. A ventilator fan was added to the housing and arranged to supply an adequate quantity of air through the system (fig. 1). This blower can be arranged to be out of action during the filament pre-heat and stand-by modes in order to prevent excessive cooling of the tube. Momentary bouts of speech (below 6 s) do not require the blower to be switched on but it was arranged to automatically operate after that period. A cool-down period of between 15 to 30 seconds (according to the length of transmission) is allowed in which the blower continues to run after the last speech syllable. A further control of the blower motor is effected by an NTC resistor affixed to the final-stage. This simple electronic method of cooling ensures that the transmitter operates stably and efficiently. The temperature at the anode connection of the PA tube did not rise above 40° even after a prolonged period of operation.

Similar increases were not required for the cooling of the penultimate stage, but nevertheless, the YD 1060's heat-sink was replaced by two 2C39 heat-sinks connected mechanically together (fig. 2). Following this alteration the driver at 6 W output was adequately cooled by a very small blower. Details of the cooling arrangements may be seen in the photographs of **figs. 14, 15 and 16.**

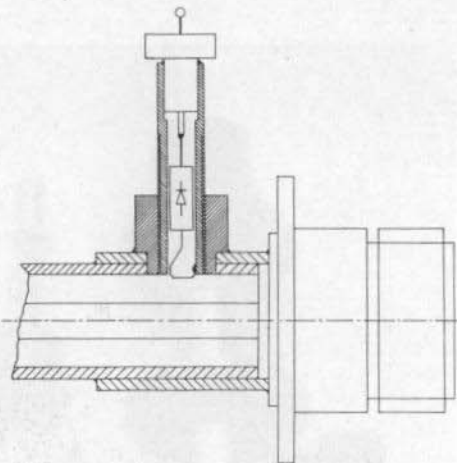


Fig. 13: Output detector probe; diode = general microwave type (but HP 2800 will just suffice), C = 1 nF

1.6. Power Display

For many radio amateurs, the arrangements necessary to monitor the power output seem to involve some difficulties. At first sight, it may appear that a directional coupler inserted in the antenna output line would be an indispensable component for this purpose. A well-tryed, simple, but effective alternative is the diode detector probe which is located in the output line. It can be fitted with a moving-coil meter reading DC milli-amps and calibrated against other devices such as a power meter, for example. Details of the detector probe may be seen in **fig. 13.**

2. CONCLUSION

As opposed to the power amplifier, the driver stage gave no great problems in its construction. Despite the lower working frequency, the power output was lower by some 1 or 2 dB than that obtained at 6 cm. This was attributed to the barely sufficient arrangements for the driver anode capacitance which can, of course, be regarded as a weak point in the design. The power output at

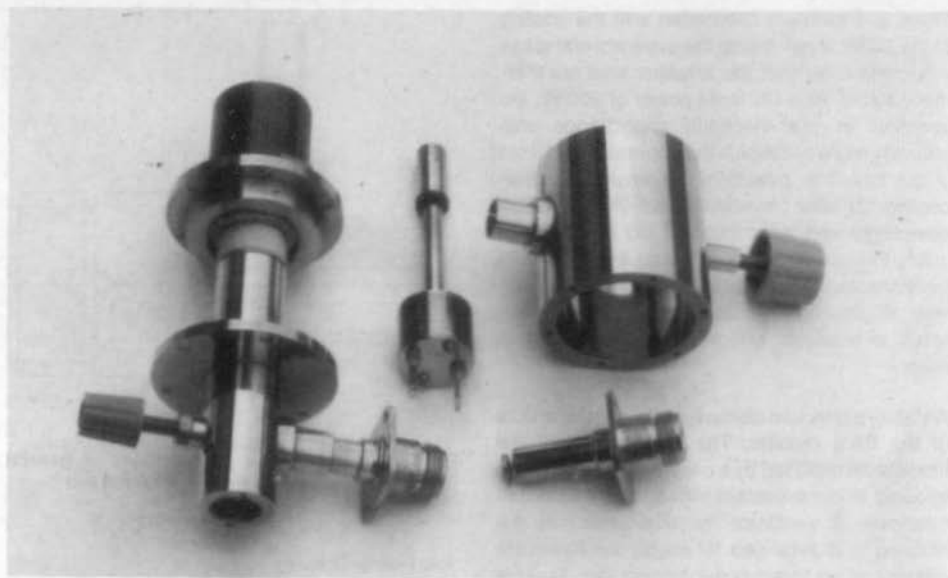


Fig. 14: The 2C39 PA dis-assembled

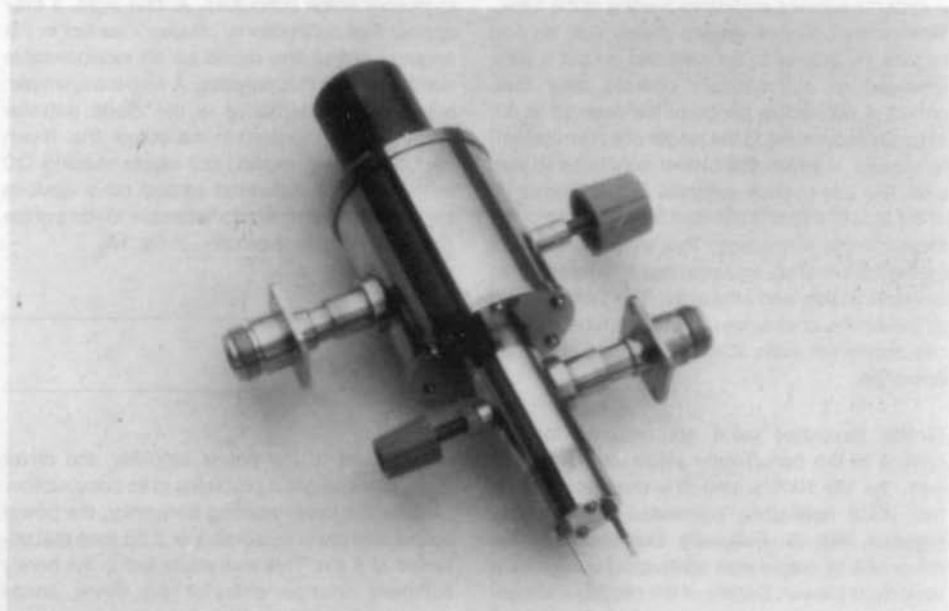


Fig. 15: The assembled 2C39 PA

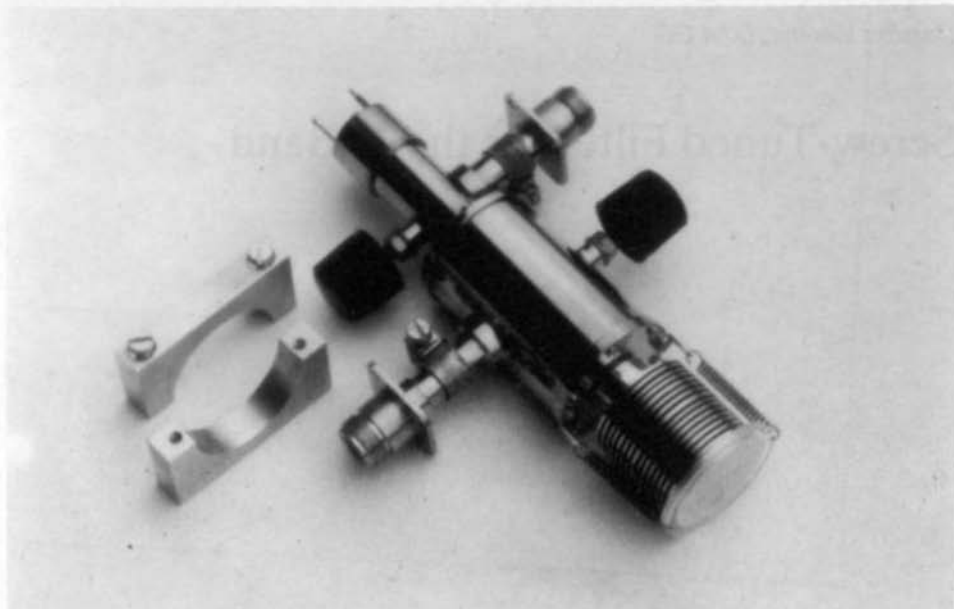


Fig. 16: YD 1060 PA with mounting cradles

8 W with 14 dB gain was easily achieved and it was possible to obtain a maximum of 12 W at 11 dB gain. The efficiency, at 25 %, necessitated the use of only a very small cooling blower to assure a completely stable operation.

The power amplifier operates with an unloaded voltage of 950 V. At 6 W drive power, the anode current rises from a quiescent 50 mA to some 350 mA. This gives a DC input power of 300 W and a measured RF output of 65 W.

Of course, thermally induced power instabilities were in evidence at this power output but even at sustained outputs, the power never dropped to below 90 % of its maximum value. Spurious outputs were measured at -80 dBc – barely detectable. Both of these amplifiers have now been in operation for 1 1/2 year and have withstood the rigours of several contests without any problems.

Special thanks are due to Rolf Küppers, DL 4 JK, who carried out the measurements on both PAs using commercial test equipment. The photo-

graphs were taken by Horst Lehrke and the author did the drawings.

3. REFERENCES

- (1) Roman Wesolowski, DJ 6 EP:
5760 MHz Power Amplifier using the YD 1060
VHF COMMUNICATIONS Vol. 19,
ed. 4/1987, p. 204 - 209
- (2) Horst Burfeindt, DC 9 XG:
A SSB Transmit Mixer and Linear Amplifier
for 3456 MHz
VHF COMMUNICATIONS Vol. 16,
ed. 1/1984, p. 13 - 22
- (3) Franz R. Rathenow, DF 9 ZT:
Oil Cooling for High-Power Tubes
VHF COMMUNICATIONS Vol. 18,
ed. 1/1986, p. 41 - 46



Carsten Vieland, DJ 4 GC

Screw-Tuned Filter for the X-Band

It is astounding the things that one can do with M3 screws! A successfully completed printed circuit board can be fastened into its case and an moonshiner's exploded boiler can be repaired using these tiny helpers. They are even to be found as fashion accessories in the ear-lobes of punkers, complete with locking nuts as insurance that they do not fall out in a hurry. Who would have imagined, however, that these unlikely examples of their utility could be outdone by their use as microwave resonators. The following article will describe the construction of a microwave filter which uses M3 screws as the selective elements.

Many publications have already described methods of selection for the 10 GHz region. If now another species is added to the existing well-known ones, such as cavity filters and stripline resonators, it should be differentiated by either its electrical data or its method of fabrication. With the exception of the SMA input and output connectors, all the necessary material for this project may be obtained from the local hardware store. The cheap and easy construction together with the facile alignment procedure should stimulate an

immediate urge to get to grips with this project.

There are two basic types of filter structures, the finger arrangement (i.e. resonators arranged on one side of the cavity) or the inter-digital (i.e. resonators arranged on both sides of the cavity). One could also consider the perpendicular positioned resonators but they exhibit, for the most part, only capacitive coupling between each resonator element. For the same bandwidth, the finger structure is always the physically shorter, and is therefore to be preferred.

The degree of coupling between the resonators is, in the first approximation, a function of the proximity of the posts to one another. Critical, and greater coupling factors, can result in bandwidths of up to 500 MHz whereas under-critical couplings of similar dimensioned posts can produce 3 dB bandwidths of only 20 MHz. It can be used to suppress a local oscillator at 10.3 GHz, which is only removed from the signal frequency by 145 MHz, by some 30 dB; the image frequency, 290 MHz away, being suppressed by 40 dB — albeit at the cost of increased insertion loss.

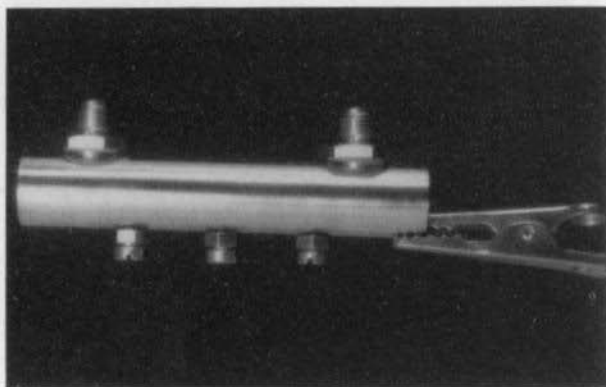


Fig. 1:
Completed resonator filter
with SMA sockets

1. MECHANICAL CONSTRUCTION

The individual resonators of the finger or interdigital filter for say, the 23 cm band, have a mechanical length of about 10 to 20 % below $\lambda/4$. The fine-tuning is carried out by capacitive loading (screws) at the hot end. The resonators, discussed here, consist of only screws and protrude equally from the cavity wall. A $\lambda/4$ at 23 cm is 8 mm long.

The filter housing should not offer much more space than absolutely necessary to accommo-

date the screw resonators, otherwise, there could be a possibility of mode changes occurring. A particularly favourable type would be of circular cross-section, as the cut-off frequency of the lowest stable mode for round waveguides lies considerably above those of rectangular cross-section. In the following constructional example, a standard brass tube of 12 mm external, and 10 mm internal diameter, is employed. The lowest cavity transmission frequency for this type of tubing lies above 20 GHz. The 1 mm wall thickness is sufficient for a stable M3 screw-thread to be cut (fig. 1).

It has been found in practice, that the M3 brass screws which have been polished with steel wool

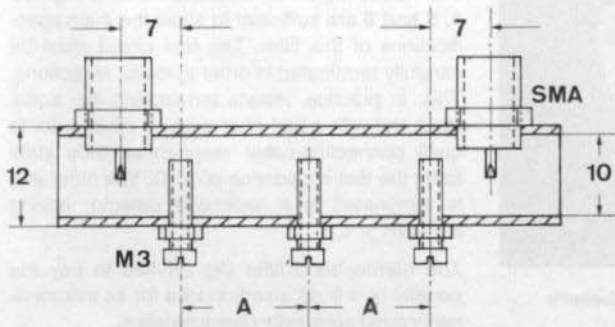


Fig. 2:
Cross-sectional view of X-band
finger filter

filter	bandwidth MHz	insertion- loss/dB	spacing A/mm
1	20	9	18
2	80	2.5	15
3	110	2.5	13
4	220	1	10

Table 1: Results for the 4-stage versions

and then plated with rubbing silver, possess a higher Q than untreated screws. Treating the inside of the brass tube, however, results in only a small improvement. In order to guard the treated screws against subsequent corrosion they must be cleaned carefully with a brush and hot water.

Figure 2 shows the principle of construction of this filter: for the dimension A can be found four examples in table 1. The distances A of the resonators' spacing were dimensioned according to cut-and-try methods. In principle, a smaller



Fig. 3: Coupling by means of the SMA-socket's spigot

spacing increases the bandwidth. The upper limit of the bandpass is reached when the bandpass ripple becomes unacceptably high. A 450 MHz wide filter (undocumented) should just about mark the absolute limit.

The under-critically coupled example, shown in fig. 6, represents what this technique can yield in the way of selectivity. The circuit Q is over 500 and there is a great possibility of the circuit being de-tuned under the influence of varying temperature, oxidization or the aging of the materials.

The SMA sockets (SMC is just as usable) are screwed in. The method of doing this may be clearly seen in fig. 3. As the thread is 3/8", many builders in Europe may not easily acquire a set of taps to cut the thread and it may therefore be expedient to solder the socket in. The hole in the tube has a diameter of 2.75 mm for an impedance of 50 Ω . If the spigot is teflon covered, the hole diameter is then 4.1 mm. The length of the coupling spigot is not too critical, being somewhere between 3 and 4 mm.

With the aid of nomograms (unavailable to the author), all the important parameters may be easily obtained without having to calculate them. This, more exact approach, will result in the insertion-loss being a little smaller. The ends of the tube can be, but need not be, capped.

2. MEASUREMENT RESULTS

The frequency swept measurements of figures 4, 5 and 6 are sufficient to show the main specifications of this filter. The test circuit must be carefully terminated in order to inhibit reflections. This, in practice, means terminating the signal input end with a pad of at least 10 dB in order to quell connecting-cable resonances thus stabilizing the test impedance at 50 Ω . The other end is terminated in a wideband detector having a VSWR \leq 1.2.

The narrow-band filter (fig. 6) has to pay the penalty of a 9 dB insertion loss for its extraordinarily good selectivity characteristics.

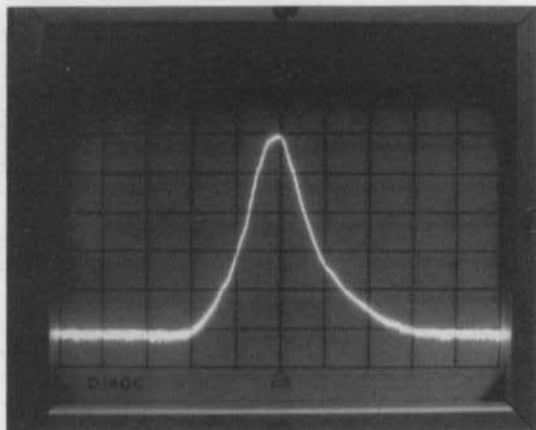


Fig. 4:
Selection characteristics of the
200 MHz wide 10.3 GHz filter
 $h = 500 \text{ MHz/cm}$, $v = 10 \text{ dB/cm}$

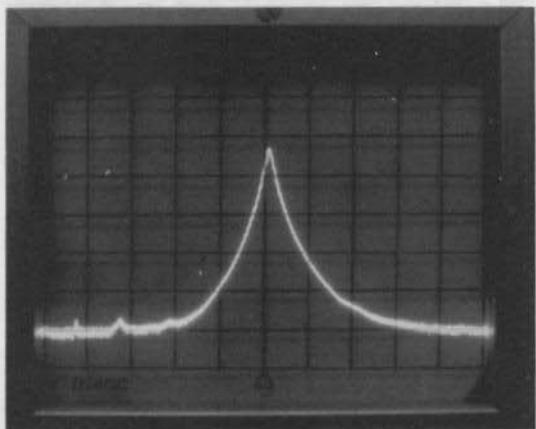


Fig. 5:
Bandwidth approx. 80 MHz
at 10.3 GHz
 $h = 250 \text{ MHz/cm}$, $v = 10 \text{ dB/cm}$

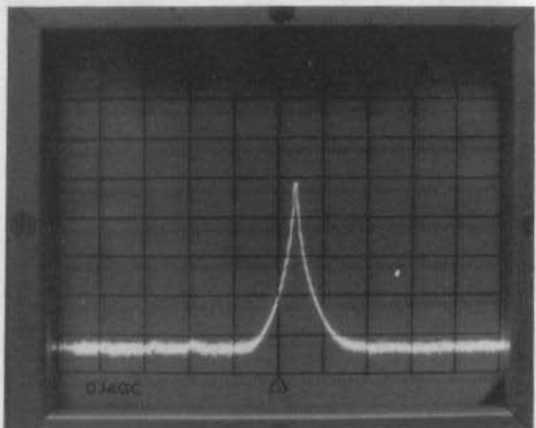


Fig. 6:
Only using a higher resolution the
3 dB bandwidth of only 20 MHz is
measurable at 10.3 GHz
 $h = 250 \text{ MHz/cm}$, $v = 10 \text{ dB/cm}$

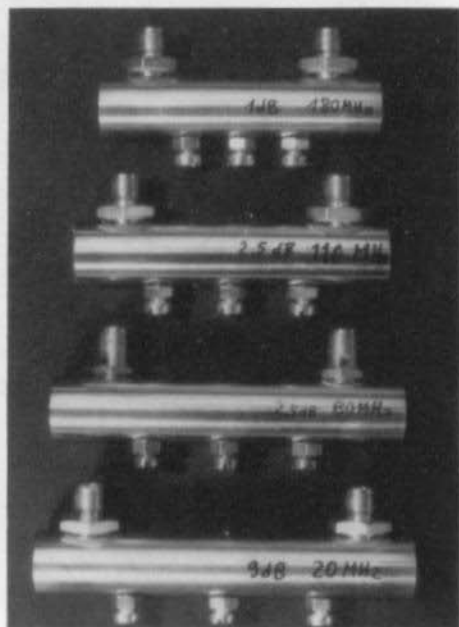


Fig. 7: "Still life" in brass

The three narrow-band versions can be aligned by simply adjusting for maximum output at 10.3 GHz. Filters having bandwidths of over 200 MHz can only be satisfactorily aligned, for minimum insertion-loss consistent with low ripple, with a 10.3 GHz sweeper test set-up.

A 5-stage version of this filter resulted in better selectivity characteristics but no improvements in the bandpass region and at the cost of increased insertion loss.

The most important characteristic of this type of filter lies in its simplicity of construction, and thereby, the amazingly short time it takes to construct and commission it. The four filters shown in **figure 7** were mechanically constructed within one hour. Apart from a vernier-gauge and the 3/8" taps, the only tools required were a drill-press and a circular-saw to cut the lengths of tubing with.

Interested in AMATEUR TV ?

....then you need CQ - TV Magazine

CQ - TV Magazine is the quarterly journal of the British Amateur Television Club. The club caters for all aspects of television including amateur transmissions, broadcast reception, video techniques, satellites, SSTV etc.

Details of membership may be obtained by sending a stamped addressed envelope to:

"BATC", 'Grenehurst', Pinewood Road
High Wycombe, Bucks HP12 4DD, U.K.



Roy Hartkopf, VK 3 AOH

Shunt-Protected Power Supply

A power-supply protection circuit is described which delivers a stabilized DC voltage and which is also adjustable. The protection covers both over-voltage and over-current conditions.

1. INTRODUCTION

In 1980, the author published (1) a short-circuit protection circuit for a low-voltage, high-current power supply. This circuit served its purpose well but was prone to an obscure failing which developed catastrophic consequences — namely a short-circuited series pass transistor. Further developments were undertaken by the author which culminated in a circuit which protects not only the connected apparatus but also the power supply itself.

2. DESCRIPTION

It is no problem to arrange over-voltage protection to a fixed-voltage power supply. It can easily be accomplished with a zener diode having a break voltage which is somewhat higher than the supply's rated output voltage. When the output voltage is variable, however, this approach can-

not be made. One practical possibility is to use any small, but sudden, increase in the output voltage to shut down the power supply.

The circuit of **fig. 1** contains both protection requirements: for an over-voltage and for a short-circuit current.

A small LF transformer is taken and given a new primary winding: a single turn of lacquered copper wire (CuL) of 2.5 mm dia. This winding is connected between the power transformer secondary and the bridge rectifier. The LF transformer's secondary winding produces a rectified negative pulse which cuts the transistor Q1 off under a pre-determined potential. The potentiometer P1 in the LF transformer's secondary enables a close control over Q1's switch-off potential — especially as the adjustment range is made smaller with R1. The diode D1 ensures that negative pulses arrive at Q1's base, and D2 suppresses the positive half-waves. Resistor R2 causes a potential drop which adds to the voltage across D2 thus making Q1 conductive in normal operation. This means that Q2 is normally cut-off.

The transistor Q1 can be cut-off by a rectified negative pulse from Q3 via C2. In normal operation, Q3 is cut-off as its base is connected to ground via a 5 M Ω resistor. Its base is connected via C1 to the output of the stabilized voltage. When (if) this voltage suddenly rises, by at least 0.7 V, Q3 conducts and cuts off Q1. This process is independent upon the actual value of output voltage. A voltage of 1 V is dropped across D3 and D4 which is sufficient to shut the circuits down when push-button switch SW 1 is



Werner Rahe, DC 8 NR

9 cm-Band Power-FET Linear Amplifier

The following article describes a two-stage amplifier module which is able to deliver an output of 0.5 W and has a gain of at least 23 dB. It is therefore very suitable for portable use after an output digital filter (1) has been added. The respectable output power is also sufficient to drive a disc-seal triode using valves such as the YD 1060 (Telefunken) or the RH7c (Siemens).

1. CIRCUIT DESCRIPTION

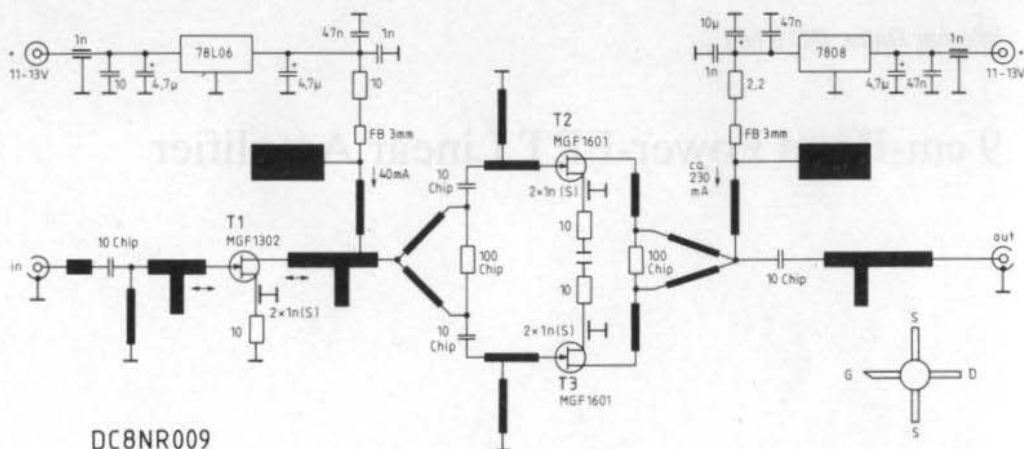
There is no longer a sufficient supply of efficient, but at the same time, reasonably priced silicon semi-conductor devices available for the 9 cm band. It would seem worth-while, therefore, to place several small-signal transistors in parallel as proposed in (2) in order to achieve the required output power. This power amplifier, however, has all its transistors working at the limits of their ratings (BFG 91 A: $I_{CAV} = 35$ mA!) and despite all the trouble taken, it still worked in the saturation area at full output power. The small stage gain of 3 to 4 dB with four parallelised transistors is a sure indication of this.

In the proposed amplifier, GaAs-FETs are used (fig. 1), the driver stage being the well-known MGF 1302. The final stage uses two power FETs, MGF 1601, working in parallel but isolated inputs and outputs (from each other) by a Wilkinson divider (3). Experiments have shown that this method of working is the most efficient due to the definite impedance ratios which can be obtained.

In the interests of linearity, all stages work in class A. Thermal runaway is not possible with FETs as they possess a negative temperature coefficient. This is not the case with bipolar devices, however.

Automatic bias is used for the FETs in order to place the gate at a negative potential with respect to the source. The source's decoupling must be carried out carefully, using plate capacitors, to ensure a good RF ground with low inductance. This will pay off in terms of amplifier stability and gain. As the test data indicates, this method of biasing does not involve any real disadvantages at these frequencies compared to direct source grounding.

The MGF 1601 has been available for some time now, it is quite cheap and the manufacturers claim an output power, at 8 GHz, of 150 mW (1 dB compression) and at 6 to 8 dB gain ($V_{DS} = 6$ V, $I_D = 100$ mA). At about an octave lower, the performance will be even better.



DC8NR009

Fig. 1: Two-stage 9 cm-band power amplifier using GaAs-FETs

2. CONSTRUCTION

The circuit is constructed upon a 0.79 mm thick, double copper-coated printed circuit board (DC 8 NR 009) using a PTFE substrate. It has the dimensions 72 x 72 mm and fits into a proprietary tin-plate box 74 x 74 x 30 mm.

The placement of the (few) components on the board (fig. 2) is, with the exception of the source decoupling capacitors, uncritical. Further information is given in more detail in figs. 3 and 4.

The distance between the two holes for each transistor is determined by the diameter of the plate capacitors used. These capacitors should be as small and as thin as possible (lightly coloured ceramic material). The PCB pattern and hole placement should be regarded as being merely a guide, the actual pattern depending upon the components to hand. The holes should be drilled, first of all, with a small drill and then filed out so that there is a 2 mm separation between the circumference of the holes for the MGF 1302, and 2.8 mm for the MGF 1601. The capacitors

should be able to be inserted with a push fit, therefore care is required in the filing-out process!

In addition, both final transistors have a 2.8 mm wide slot filed out between these holes. This will accept the transistor body at a later stage.

This slot is now covered on the track side with a piece of copper foil 0.5 to 0.8 mm thick.

To do this, the track is thinly tinned at the appropriate places and the tinned foil is then pressed down onto the board with the hot soldering iron.

Using a soldering iron temperature of 450° C, the high heat conductivity of copper will ensure that this operation will be completed quick enough to avoid damage to the copper track side of the board.

Finally, the plate capacitors are placed in the appropriate holes and soldered in using the same technique as with the copper foil.

The printed circuit board may, by this time, be a little buckled and should now be carefully straightened out before it is soldered into its previously prepared tin-plate housing. Care should be taken that the socket pins fall exactly upon the appropriate pads in order that they

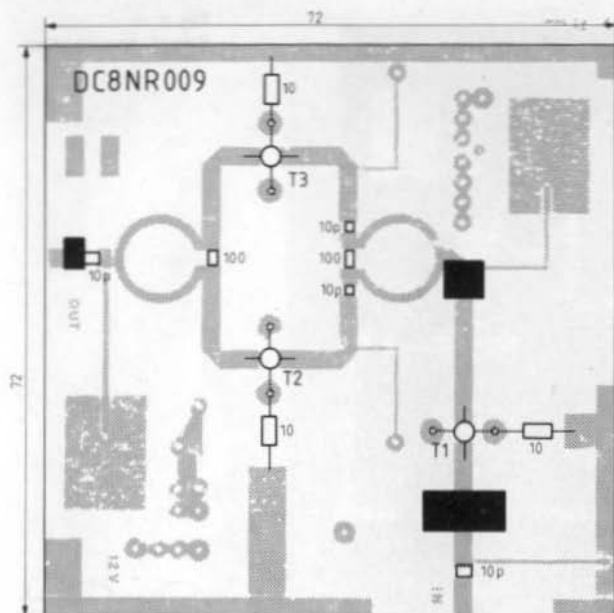


Fig. 2a:
RF component location
on the track side of the
PCB

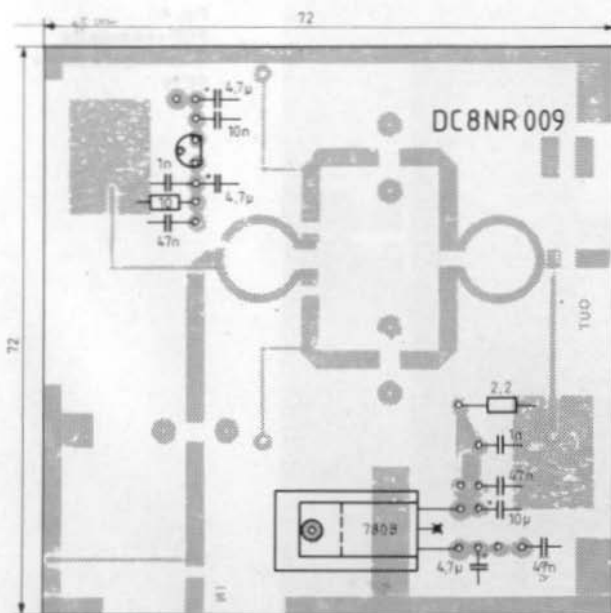


Fig. 2b:
DC component location
on the ground plane of
the board

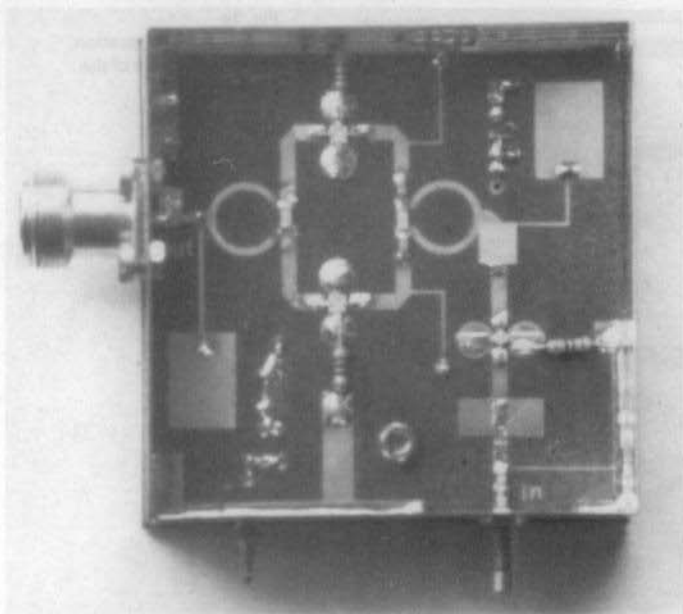


Fig. 3:
Sample construction

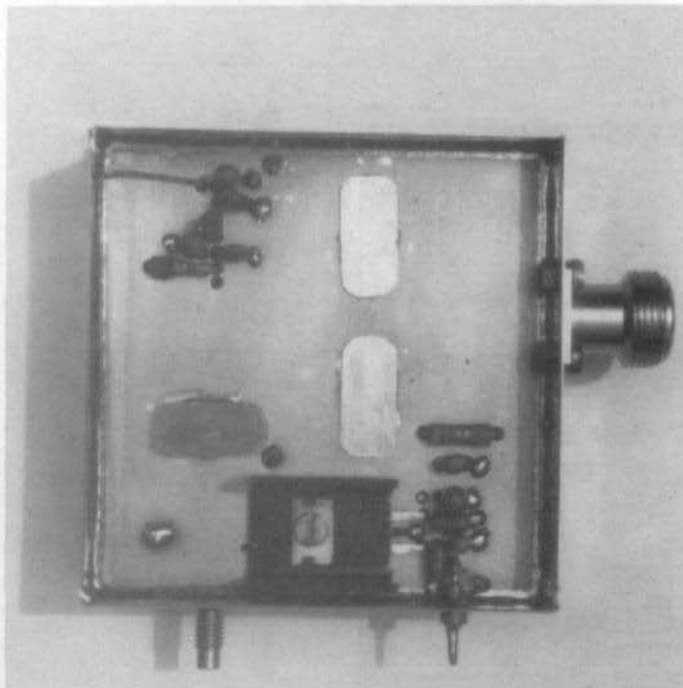
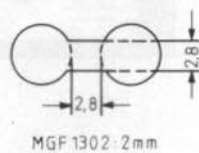


Fig. 4:
PCB cut-outs for
mounting the power
FETs





can be soldered directly to the track side of the board.

These connectors' inner conductors should also be shortened before fitting and the PTFE collar removed as far as possible. If N-connectors are used, it is better to use the precision version. This has a smaller flange than the standard version and require only a 4 mm mounting hole to be drilled. They also have a better match to the board transmission lines. The coupling capacitors used were all high-Q types with a light-coloured ceramic substrate.

3. SETTING UP

Before soldering in the semi-conductors, the voltage at the output of the voltage regulators should be checked.

On account of the relatively high dissipation of heat from these output devices, they must be sufficiently cooled. This is accomplished by pressing in the transistors, with the markings underneath, into the slots provided in the board. The transistor leads are then soldered on to the tracks. A little heat paste will ensure better heat conductivity.

Whilst the gate and drain leads are cut off so that only 3 mm remains, the source connection is snipped off only so that it does not project beyond the plate decoupling capacitor. During the mounting phase, the usual precautions must be followed to prevent high static electrical charges from accumulating across these expensive transistors. Also the inputs and outputs must be directly terminated during the tuning process in order to prevent a mismatch occurring due to a high VSWR at the end of the test cables. Pads of 3 dB or more should be suitable for this purpose.

Directly following the application of the supply voltage, the quiescent current given in the circuit diagram should be set. This value should only slightly increase when drive is applied. The symmetry of the output stage is then checked by

measuring the potential differences across the source resistors. These voltages must only differ from one another by only a few millivolts, whether drive is applied or not.

If the devices come from the same batch, as was the case with the author, then there will be no difficulty with the symmetry. If balancing is necessary, however, it can be done either by changing source resistors or a small capacitive tuning-foil soldered to the source lead.

The tuning procedure consists of gripping a small piece of copper foil with a cleft matchstick, sliding it up and down and in contact with the tracks, and watching for the largest peak in output power. The foil is then soldered to that position using as little solder as possible. This procedure is carried out three times. The dimensions of the foil strips and their distances from the device connections are: —

Gate:	6 x 13 mm, distance \approx 7 mm
Drain:	5.5 x 7 mm, distance \approx 10 mm
Output:	4 x 4 mm

These dimensions should be regarded as being for guidance only, a little experimenting with different foil sizes and distances may result in a few more tenths of a dB output power.

4. TEST RESULTS

This two-stage module has, for this frequency range, an astoundingly high state gain. It amounted to some 28 dB for an output power of 0.5 W. The 1 dB compression point lies somewhat under this power. Higher drive then results in saturation. Nevertheless, 0.7 W with a gain of 24 dB was achieved. Input drive powers of more than 2 mW are to be inhibited by means of input attenuator pads.

The final transistors are stable, even when working under changing load conditions, and also putting on the cover caused little change. To ensure a good heat exchange, it is perhaps advisable not to put a cover on the component



side. Another, alternative, measure is to perforate the cover over the voltage regulators.

5. ACHIEVING MORE POWER

Whilst a power of around a half watt is obtained at a moderate cost, the extraction of yet higher powers is fraught with considerable trouble. It is only worth-while if such an increase results in a gain of some 6 dB (an S-point) for working in over-the-horizon conditions.

The construction of a valved power amplifier is also time consuming and mechanically tedious. In the absence of a talent for mechanical work and also the necessary machine tools, no real progress can be expected.

Even with careful construction, valved amplifiers tend to detune owing to the action of heat upon high-Q resonators and inter-electrode capacitances. This effectively rules out their use anywhere near an antenna. In any case, the author has not yet constructed, or even seen, any example of a valved amplifier which, during intermittent operation, is absolutely stable – in continuous operation certainly. Compensation circuits working air-cooling blowers are of little help owing to their inertia (4). Over-ambitious expectations are definitely misplaced taking this route.

GaAs-FETs do offer a power gain of some 10 dB in this frequency range, at powers approaching

6 W. This type of device is, however, for the communications bands, internally designed for 50 Ω matching and expensive (> 1 kDM). Possibly it may be worth-while to employ these devices in a few instances as such a stage will be able to operate with pre-amplifier and change-over relay and be located directly in the vicinity of the antenna thus avoiding large feed-cable losses.

6. REFERENCES

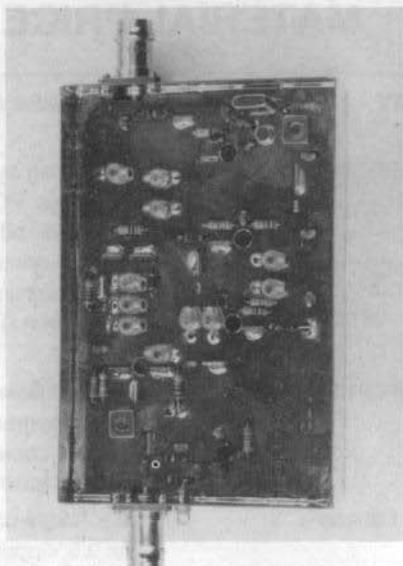
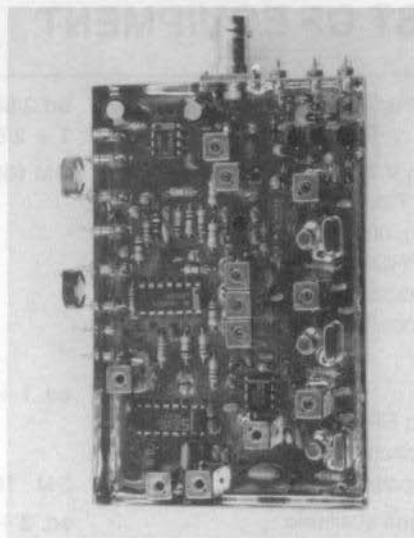
- (1) Burfeindt, H., DC 9 XG:
A SSB Transmit Mixer and Linear Amplifier for 3456 MHz
VHF COMMUNICATIONS, Vol. 16,
ed. 1/1984, p. 13 - 22
- (2) Team of authors:
Ein 9 cm Transvertersystem moderner Konzeption
CQ-DL 9 - 11/88
- (3) Hupfer, K., DJ 1 EE:
Wideband Power-Divider/Combiner for the 2 m and 70 cm Bands
VHF COMMUNICATIONS, Vol. 20,
ed. 1/1988, p. 2 - 7
- (4) Wesolowski, R., DJ 6 EP:
9 cm-Band Tube PA Stage
VHF COMMUNICATIONS, Vol. 21,
ed. 4/1989, p. 232 - 241



MATERIAL PRICE LIST OF EQUIPMENT

YT3MV	DSP Computer for Radio Amateur Applications	Art.No.	ed.2/88, 1 + 2/89
Set of PCBs, progr. EPROM, operating system V.7.2.		6004	DM 1050.00
	Contains: PCBs YT3MV 003 (bus), 004, 005, 006 (4 x), 007, 008 and 009; a programmed EPROM, a set of copies of all diagrams and component lay-out plans (in A4), the operating-system manual.		
YT3MV 010	Interface for KR-5600 Rotators		ed. 1 + 2/89
	PCB, programmed EPROM, together with A4 copies of circuit schematics and component location plans	6003	DM 100.00
User software	4 software packages available on 3.5" floppy		ed. 3 + 4/89 each DM 45.00
	on 5.25" floppy		each DM 50.00
	List upon request!		
DCØDA	10 GHz Transverter System "microline 3"		ed. 2 + 3/89
XLO-1	Oscillator		ed. 2/89
Kit	contains all original components listed in chapter 2.3.	6601	DM 178.00
Module	ready-to-operate	S 3030	DM 220.00
Option 01	with stab. crystal (TK 10 ppm), temp.-compensation	S 3031	DM 270.-
XRM-1	Receive mixer		ed. 3/89
Kit	Contains all original components listed in chapter 3.3.	6603	DM 345.00
Module	ready-to-operate	S 3032	DM 445.00
XTM-1	Transmit mixer		ed. 3/89
Kit	Contains all original components listed in chapter 4.3.	6605	DM 355.00
Module	ready-to-operate 100 mW	S 3033	DM 480.00
Option 01	200 mW	S 3034	DM 575.00
Original Johannson trimming tool for μ W trimmer		6607	DM 18.50





A new METEOSAT converter as a compact kit

Description in VHF COMMUNICATIONS 1/1990

- * Input frequencies: 1691.0 and 1694.5 MHz
- * Intermediate frequencies: 137.5 and 134.0 MHz
- * NF = 1.7 dB (typ); G = 26 dB (typ)
- * Operation voltage 12 - 14 V, approx. 80 mA
- * Dimensions (mm): 111 x 74 x 30 and BNC socket

The matching weather-satellite receiver

- * 3 channels: 134.0/137.5 and 137.62 MHz
- * Sufficient sensitivity for direct NOAA reception on 137.5 and 137.62 MHz
- * Operation voltage 12 - 14 V; Connections for loudspeaker, S-meter, channel-switch
- * Dimensions (mm): 111 x 74 x 30 and BNC socket

Special offer (in stock)

	Art.No.	Price
Converter, kit with all components	6510	DM 395.00
Converter, ready-to-operate module	3029	DM 575.00
Receiver, kit with all components	6511	DM 445.00
Receiver, ready-to-operate module	3310	DM 925.00



UKWberichte T. Bittan OHG · Jahnstr. 14 · P.O.Box 80 · D-8523 Baiersdorf

Tel. West Germany 9133 47-0. For Representatives see cover page 2



Plastic Binders for VHF COMMUNICATIONS

- Attractive plastic covered in VHF blue
- Accepts up to 12 editions (three volumes)
- Allows any required copy to be found easily
- Keeps the XYL happy and contented
- Will be sent anywhere in the world for DM 10.00 including surface mail

Order your binder via the national representative or directly from the publishers of VHF COMMUNICATIONS (see below)

Prices for VHF COMMUNICATIONS

Subscription	Volume	Individual copy
VHF COMMUNICATIONS 1990	DM 27.00	each DM 7.50
VHF COMMUNICATIONS 1988 to 1989	DM 25.00	each DM 7.50
VHF COMMUNICATIONS 1986 to 1987	DM 24.00	each DM 7.00
VHF COMMUNICATIONS 1985	DM 20.00	each DM 6.00
VHF COMMUNICATIONS 1980 to 1984	DM 16.00	each DM 4.50
VHF COMMUNICATIONS 1975	DM 12.00	each DM 3.50
VHF COMMUNICATIONS 1976 to 1979 (incomplete, only 3 editions)	DM 9.00	each DM 3.50

Individual copies out of order, incomplete volumes, as long as stock lasts:

2/1971, 1/1972, 2/1972, 4/1972,

2/1973, 4/1973, 1/1974, 2/1974

each DM 2.00

each DM 2.00

Plastic binder for 3 volumes

DM 10.00

We shall not be able to reprint editions which are older than 6 years.

All prices including surface mail

When ordering 3 complete volumes, a free binder is included!



UKWberichte Terry D. Bittan · Jahnstr. 14 · Postfach 80 · D-8523 Baiersdorf

Tel. West Germany 9133 47-0. For Representatives see cover page 2

Ultimate long-term stability



We deliver:

Oven controlled Crystals oscillators (OCXO)

Electronic components for
the highest requirements

Crystals
Filters
Oscillators

OCO 100, OCO 110, OCO 120
TQOC 5-02

- short power-up time, OCO 100: 2,5 min (25 °C)
- low current consumption
OCO 100: 50 mA/25 °C
- low profile, OCO 100: 16,5 mm resp. 19,4 mm
OCO 110: 15 mm
- highest stability, TQOC 5-02: $TK < \pm 5 \cdot 10^{-9}$
- ageing, TQOC 5-02: $< \pm 5 \cdot 10^{-9}$ /year

TELE QUARZ

TELE-QUARZ GMBH
Landstraße
D-6924 Neckarbischofsheim 2
Telefon 0 72 68/8 01-0
Telex 782 359 tq d
Telefax 0 72 68/14 35